A NEW 6 MV TANDEM ACCELERATOR FOR ACCELERATOR MASS SPECTROMETRY, ION BEAM ANALYSIS AND HIGH-ENERGY ION IMPLANTATION AT FZD. Sh. Akhmadaliev, S. Merchel, A. Kolitsch, W. Möller, Forschungszentrum Dresden-Rossendorf, Institute of Ion Beam Physics and Materials Research, D-01314 Dresden, Germany, E-mail: akhmadaliev@fzd.de

A new 6 MV tandem accelerator is put into operation at FZ Dresden-Rossendorf (FZD). This opens a new field of research at FZD: accelerator mass spectrometry (AMS). The Dresden AMS facility (DREAMS) will especially be used for measurements of ^{10}Be, ^{26}Al, ^{36}Cl, ^{41}Ca, and ^{129}I in the isotopic ratios in the range of 10^{-10} - 10^{-16}. The accelerator will be also used for ion beam analysis such as RBS, ERD, PIXE/PIGE, and NRA as well as for materials modification via high-energy ion implantation.

The system is based on a medium current 6 MV-Tandetron™ produced by High Voltage Engineering Europe (HVEE). It operates via a Cockcroft-Walton type high voltage generator providing the terminal voltage up to 6 MV. The accelerator has two separate ion injection systems as well as two high-energy 90° analysing magnets (Fig. 1).

The AMS injector consist of two Cs-sputter ion sources (SO-110) with wheels for up to 200 samples (Fig. 2) each, a 54° electrostatic analyser (ESA) and a 90° bouncer magnet for sequential acceleration of the stable and radionuclides. The high-energy part of the system comprises a 90° analysing magnet, a set of Faraday cups with energy slits for measuring the stable nuclides and stabilising the terminal voltage, a set of post-stripper silicon nitride foils for isobar suppression, a 35° ESA, and a 30° vertical magnet for further suppression of interfering species. The radionuclides will be registered by a 4-anode ΔE/E gas ionisation detector [1].

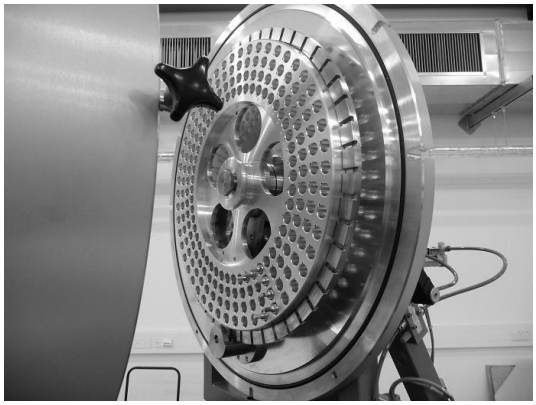

Fig. 2: One of the two sample wheels for 200 AMS targets.

The accelerator is additionally equipped with a multipurpose ion injector (MPI) containing a Cs-sputter ion source and a He-duoplasmatron for high-energy ion implantation in the automatic wafer-handler and for ion beam analysis. The interconnecting beamline will connect the new system with the existing experimental equipment at 5 MV-Tandem accelerator via two 90° magnets.

References: [1] Arnold M. et al. accepted for *Nucl. Instr. and Meth. B* (Proceedings of IBA2009).

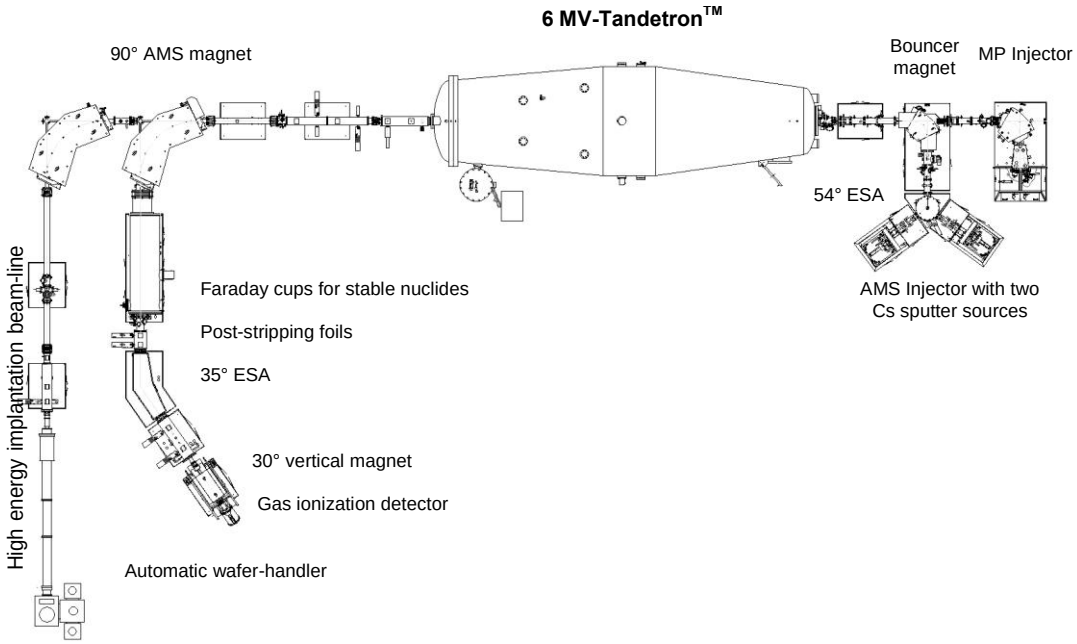

Fig. 1: AMS facility (DREAMS) at FZD.

ION BEAM INDUCED LUMINESCENCE IN n-TYPE ZnO. M. Allardt[1], R. Stübner[1], Vl. Kolkovsky[1], D. Severin[2], M. Bender[2] and J. Weber[1], [1]Technische Universität Dresden, 01062 Dresden, Germany, [2]GSI Helmholtzzentrum für Schwerionenforschung, 64291 Darmstadt, Germany

Luminescence induced by Au ions of 4.8 MeV/amu has been studied at different temperatures in n-type ZnO. Two dominant bands at about 400 nm and 500 nm respectively were observed at room temperature. The intensity of these bands decreases as a function of the irradiation dose. On the other hand the low temperature luminescence spectra are dominated by the bands at about 370 nm and 550 nm respectively. The experimental results will be combined with the photoluminescence measurements performed after annealing at room temperature. The possible origin of the peaks will be discussed.

APPLICATION OF ION BEAM PROCESSING FOR FABRICATING HIGH-END OPTICS FROM X-RAY TO VISIBLE LIGHT. F. Allenstein, M. Zeuner, A. Luca, E. Loos, M. Nestler, Roth & Rau MicroSystems GmbH, Gewerbering 3, 09337 Hohenstein-Ernstthal, Germany

In this paper we present applications by using Broad Ion Beam Sources with a typical energy range of 100 V up to 2 kV and beam currents in a magnitude of order of about 500 mA. The tools are suitable for a very accurate deposition of thin films and multilayer structures and for ion beam milling. Typical values obtained with our technology are: deposited thickness uniformity below 0.1%, run-to-run reproducibility of 99.9% and layer micro-roughness of 0.15 nm (rms). Due to their high performance the IonSys tools are successfully used to fabricate high-end optics for a wide spectral range, from X ray to visible light.

Introduction: Ion Beam Etching (IBE) and Ion Beam Sputter Deposition (IBSD) are increasingly used for advanced applications in semiconductor technology [1], high-end optics [2] and material processing. These ion beam technologies offer two general features with respect to other conventional techniques: First, separation of the plasma generation and the deposition area results in low damage density respectively contamination and second high flexibility referring to the independent control of relevant deposition parameters (particle energy and flux density, deposition rate, process gas pressure etc.). In this paper we present applications in high-end production as well as for R&D.

EUV and X-Ray Optics: Extreme ultraviolet lithography (EUVL) is nowadays the most promising candidate for integrated circuit manufacturing with the 32 nm node and below. Due to the strongly absorption of EUV radiation at 13.5 nm in virtually all materials high-quality reflective coatings are required for optics and masks inside of exposure tools. These multilayer mirrors are formed by deposition on low thermal expansion material substrates of alternating layers, typically 50 bi-layers of molybdenum (Mo) and silicon (Si) with period thicknesses around 7 nm. The EUVL makes high demands on the multilayer deposition technique not only regarding a high reflectivity at exposure wavelength but also high layer thickness uniformity, thermal stability and a low stress. Furthermore, the defect-free mask blank deposition with defect density less than 0.003 cm^{-2} @ 25 nm is the top challenge of EUVL [3]. Since 2005 the IonSys 1600 is successfully used at Fraunhofer Institute for Material and Beam Technology (IWS Dresden) to fabricate precise multilayer mirrors for EUV spectral range. With reflectances up to 70% our IBSD technology is in the forefront of this field of application. These values near to the theoretical limit indicate a high regularity of the Mo/Si-stacks by low interfaces widths and roughness.

High-Reflectivity Distributed Bragg Reflectors for UV spectral range: In order to meet the requirements of an increasing quantity of data that must be stored, the laser wavelength in the data storage devices is continually reduced in recent years. For example, substantially more data can be stored on a Blu-ray disc than on the DVD format because of its shorter wavelength (405 nm). By further reduction of operating wavelength down to the ultraviolet (UV) spectral range a storage media over 100 GB (single layer) capacity would be possible. Therefore, efficient UV lasers are in the great interest of current research works for medical and sensor applications, too [4].

For some years technology for hybrid UV vertical-cavity surface-emitting lasers (VCSELs) with organic active material is developed at Institute of Nanostructure Technologies and Analytics (INA, University of Kassel). To fabricate the high quality optical resonator formed with distributed Bragg reflectors (DBRs) the IonSys 1000 is successfully in use. In particular, a low deposition temperature of IBSD technique makes it most suitable for devices with pre-deposited organic material. A typical DBR structure consists of multiple layers of alternating materials with varying refractive index, in this case SiO_2 as a low index material (n = 1.48) and ZrO2 as a high index material (n = 2.12). The low absorption for UV spectral range and the high refractive index contrast ($\Delta n = 0.64$ @ 380 nm) of this material system make it possible to deposit high-reflectivity UV mirrors with relatively few periods.

References: [1] Zeuner M., Nestler M., Roth D. *Vakuum in Forschung und Praxis* **19(2)** (2007) 15-20. [2] Gawlitza P., Braun S., Leson A., Lipfert S., Nestler M. *Vakuum in Forschung und Praxis* **19(2)** (2007) 37-43. [3] Rizvi S. *Handbook of Photomask Manufacturing Technology*, Taylor & Francis Group, 2005. [4] Schneider D., Rabe T., Riedl T., Dobbertin T., Kröger M., Becker E., Johannes H.-H., Kowalsky W., Weimann T., Wang J., Hinze P. *J. Appl. Phys.* **98** (2005) 043104.

Acknowledgements: We thank P. Gawlitza and S. Braun from IWS Dresden as well as V. Daneker, D. Todorov, M. Bartels and H. Hillmer from INA (University Kassel) for providing of research results and the fruitful cooperation.

SMALL ANGLE X-RAY SCATTERING FROM ION CLUSTERS IN MEDIUM ENERGY Xe-IRRADIATED SILICON. Andreas Biermanns[1], Antje Hanisch[2], Jörg Grenzer[2], Stefan Facsko[2] and Ullrich Pietsch[1], [1]Universität Siegen, Festkörperphysik, Walter-Flex Str. 3, 57072 Siegen, Germany, [2]Forschungszentrum Dresden-Rossendorf, Institute of Ion Beam Physics and Materials Research, P.O. Box 510119, 01314 Dresden, Germany, email: andreas.biermanns@uni-siegen.de

Introduction: In recent years, the creation of surface-nanostructures due to ion beam sputtering has gained much interest due to the possibility to pattern large surface areas with tunable morphologies in a short time. One kind of those nanostructures are wave-like patterns (ripples) produced by an interplay between a roughening process caused by ion beam erosion (sputtering) of the surface and smoothening processes caused by surface diffusion [1]. In this contribution we report on investigations of patterned Si(001) surfaces after irradiation with Xe-ions using ion-energies up to 70 keV. During the sputtering, an amorphous surface-layer is formed followed by an interface towards crystalline material, showing the same morphology as the surface. The structure and morphology of the amorphous layer and the amorphous-crystalline (a/c) interface were studied using synchrotron-radiation using grazing-incidence small angle scattering (GISAXS) and diffraction (GID) [2]. Here, we report on X-ray scattering experiments in order to resolve the nature bubble like defect seen in the amouphous surface layer. TEM measurements (Fig. 1) show the appearance of almost circular shaped dark contrast regions with a maximum diameter of 5 nm inside the amorphous layer. Similar spherical regions of larger size were already found in Ar-irradiated samples [3].

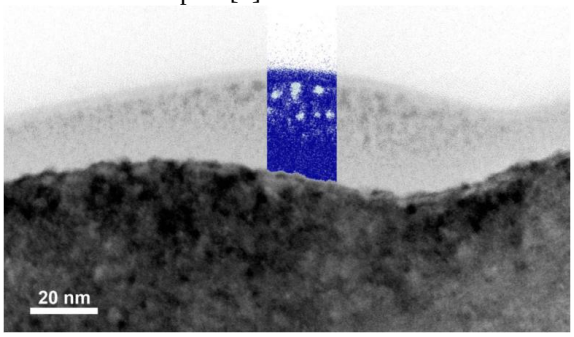

Fig. 1: TEM image of a Si surface irradiated by 35 keV Xe-ions. The amorphous region (grey) contains spherical Xe-clusters close to the surface.

One problem for the current understanding is the characterization of these structures and the determination whether they are filled with Xe/Ar or not. Although an EDX scan through the amorphous layer indicates an enhanced Xe-concentration in this layer and Rutherford backscattering measurements show the existence of Ar as well as of Xe in the corresponding irradiated samples, there is no direct evidence for the formation of Xe- or Ar-clusters as suggested by the TEM measurements.

We performed small angle X-ray scattering experiments in order to probe the size end depth distribution of those clusters. In a second step, anomalous GISAXS measurements have been used in order to verify the Xe-content of the clusters.

References: [1] Chan W.L. and Chason E. *Phys. Rev. B* **72** (2005) 165418. [2] Biermanns A. et al. *J. Appl. Phys.* **104** (2008) 044312. [3] Chini T.K., Okuyama F., Tanemura M., Nordlund K. *Phys. Rev. B* **67** (2003) 205403.

MODIFICATION OF GaAs BY Mn ION IMPLANTATION TOWARDS SEMICONDUCTOR SPINTRONIC THIN FILMS. Danilo Bürger[1], Shengqiang Zhou[1], Mukesh Pandey[2], Chebolu Subrahmanya Viswanadham[3], Jörg Grenzer[1], Olga Roshchupkina[1], Wolfgang Anwand[1], Helfried Reuther[1], Volker Gottschalch[4], Manfred Helm[1], and Heidemarie Schmidt[1], [1]Institute of Ion Beam Physics and Materials Research, Forschungszentrum Dresden-Rossendorf, Bautzner Landstraße 400, 01328 Dresden, Germany, email: d.buerger@fzd.de, [2]High Pressure Physics Division, Bhabha Atomic Research Centre, Mumbai-400085, India, [3]Materials Science Division, Bhabha Atomic Research Centre, Mumbai-400085, India, [4]Institut für Anorganische Chemie, Fakultät für Chemie und Mineralogie, Universität Leipzig, Linnéstraße 3, 04103 Leipzig, Germany

Ferromagnetic semiconductors with high Curie temperatures and large coercivity are very promising materials for spintronic applications. An approach to fabricate ferromagnetic GaMnAs is Mn ion implantation into GaAs followed by pulsed laser annealing (PLA) [1]. Magnetic Mn ions which occupy the Ga sublattice sites form acceptor centers and provide free holes for the mediation of the parallel alignment of the magnetic moments of the Mn ions. For a strong ferromagnetic interaction, activation of the Mn acceptor dopants over their thermodynamic equilibrium solubility is necessary. Long time, rapid thermal, and also flash lamp annealing processes take too long to realize a large enough free hole concentration by activation of Mn acceptor dopants. From a thermod-namical point of view, the PLA process is beside the more expensive LT-MBE process the best route to fabricate oversaturated ferromagnetic GaMnAs.

We investigated the influence of the implanted Mn concentration and PLA conditions on the structural and magnetic properties of GaMnAs thin films. We performed heatflow calculations to visualize the fast temperature quenching during the PLA process [2]. Using SQUID magnetometry, we reveal a strong decrease of the saturation magnetization with increasing number of laser pulses during PLA (Fig. 1). However, the crystalline quality is improved after several laser pulses. This has been verified by RBS (Fig. 2) and XRD measurements. The decrease of saturation magnetization after several laser pulses may be caused by the continuous Mn cluster formation during each PLA cycle.

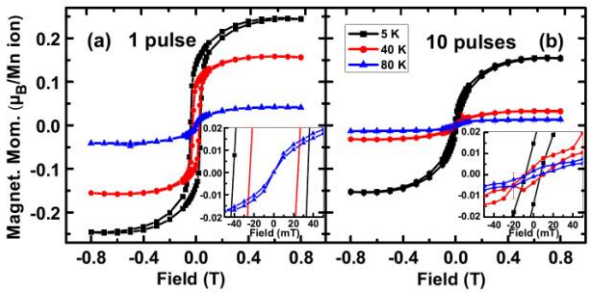

Fig. 1: Hysteresis loops of the 6 at% PLA sample measured at 5 K, 40 K, and 80 K. (a) 1 pulse. (b) 10 pulses. The insets show the region near the origin.

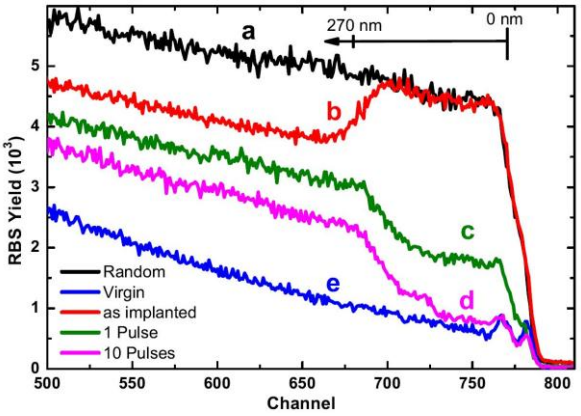

Fig. 2: RBS spectra of the implanted sample with 6 at% Mn. a-random spectrum for a virgin sample, and channeling spectra: b-as implanted, c-PLA with 1 pulse, d-PLA with 10 pulses and e-channeling spectrum of the virgin sample.

References: [1] Scarpulla M.A. et al. *APL* **82** (2003) 1251. [2] Bürger D. et al. *PRB* **81** (2010) in press.

HOMOGENEITY STUDY FOR OBSIDIAN PROVENANCING BY ION BEAM ANALYSIS. F. Eder[1], C. Neelmeijer[2], M. Bichler[1], S. Merchel[2], [1]Vienna University of Technology, Atominstitut, Stadionallee 2, 1020 Vienna, Austria, email: feder@ati.ac.at, [2]Forschungszentrum Dresden-Rossendorf (FZD), P.O. Box 510119, D-01314 Dresden, Germany

Obsidian is a natural volcanic glass which was one of the most appreciated materials by of ancient man for cutting tools and has been found by researchers in many locations, far away from any natural source. Reliable provenancing can provide evidence of contacts over a certain distance and information about exchange patterns and mobility of prehistoric people.

The application of analytical methods can solve the problem of obsidian provenancing by means of its highly specific chemical composition, the "chemical fingerprint". Combined external **I**on **B**eam **A**nalysis (IBA) measurements, consisting of **P**roton **I**nduced **X**-ray **E**mission (PIXE), **P**roton **I**nduced **γ**-ray **E**mission (PIGE) and **R**utherford **B**ackscattering **S**pectrometry (RBS), are frequently used due to the high sensitivity and the non-destructive beam mode. Our study has been carried out at the 5 MV Tandem accelerator of the Ion Beam Centre of FZD, where a number of quantitative glass analyses has been performed simultaneously with all three external ion beam techniques [1-5].

Obsidian usually exhibits a very uniform appearance and is generally described as a relatively homogeneous material. Banded obsidians can be observed also, and the question was raised, if these bands are caused by differences in the chemical composition or if these changes in the optical properties are related to inclusions of clouds of gas bubbles, microphenocrysts or similar features without significant compositional influence. Therefore, a systematic investigation of a banded obsidian sample from *Demengakion* (Milos, Greece) has been carried out in order to check the actual variation range of the chemical composition. (Fig. 1).

Fig. 1.: Banded obsidian from *Demenegakion* (Milos, Greece).

To investigate the influence of different preparation techniques on the analytical results, we produced an obsidian in-house reference sample (Fig. 2). This specimen originates from the highly homogeneous obsidian source *Hrafntinnuhryggur* (Iceland) and features three different surfaces: natural fracture, ground finish (1200 diamond lap) and polished [6].

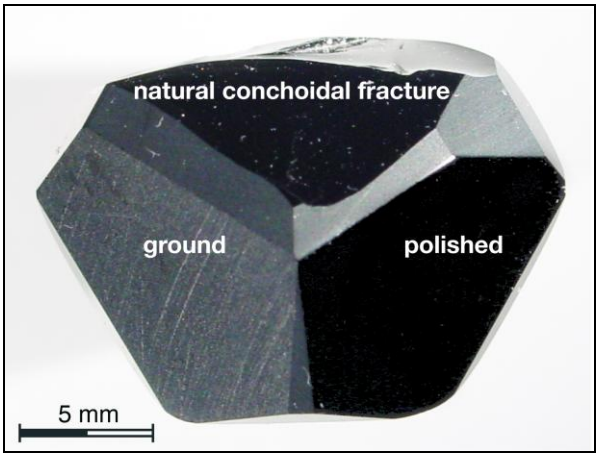

Fig. 2: Obsidian in-house reference sample with three different surface qualities.

This study is part of a project which aim is to apply selected analytical methods, in particular IBA, **N**eutron **A**ctivation **A**nalysis (NAA) and **I**nductively **C**oupled **P**lasma-**M**ass **S**pectrometry (ICP-MS), to detect a maximum of compositional differences between easily available samples of the natural obsidian sources in Europe. This knowledge should enable to decide, which least invasive analytical method should be chosen for the analysis of a specific archaeological artefact, on a case by case basis.

References: [1] Bugoi R. and Neelmeijer C. *NIMB* **226** (2004) 136–146. [2] Mäder M. et al. *NIMB* **239** (2005) 107-113. [3] Mäder M. and Neelmeijer C. *NIMB* **226** (2004) 110–118. [4] Jembrih D. et al. *NIMB* **181** (2001) 698–702. [5] Mäder M. et al. *NIMB* **136-138** (1998) 863–868. [6] Tuffen H. and Castro J. M. *Journal of Volcanology and Geothermal Research* **185** (2009) 352–366.

SURFACE MODIFICATIONS INDUCED BY SLOW HIGHLY CHARGED IONS IN CaF_2(111) AND BaF_2(111). A.S. El-Said[1], R. Heller[1], R.A. Wilhelm[1], S. Fascko[1], F. Aumayr[2], [1]Institute of Ion Beam Physics and Materials Research, Forschungszentrum Dresden-Rossendorf, P.O. Box 510119, D-01314 Dresden, Germany, [2]Institute of Applied Physics, Vienna University of Technology, A-1040 Vienna, Austria

Topographic surface modifications by single ion impacts in a given material are strongly correlated to ion-energy deposition. It has been shown that swift heavy ions (MeV-GeV) can create nano-sized features on various solids surfaces [1,2] above a critical value of the electronic energy loss *dE/dx*.

The surface nanostructures created by swift heavy ions are usually accompanied by unwanted damage inside the bulk. This limitation has been recently overcome by using slow (eV-keV) highly charged ions (HCI). By increasing the charge state, a large amount of potential energy can be stored in a HCI. This potential energy is then deposited in a nanometric volume close to the surface [3,4].

Recently, we have shown that hillock-like surface nanostructures on CaF_2 single crystals can not only be created by swift heavy ions but also by slow HCI, as long as these ions are sufficiently highly charged [5], see Fig. 1. Surprisingly, instead of a critical *dE/dx*, hillock formation by HCI exhibits a sharp potential energy threshold around 12 keV [6], which slightly increases with the ion's kinetic energy [5].

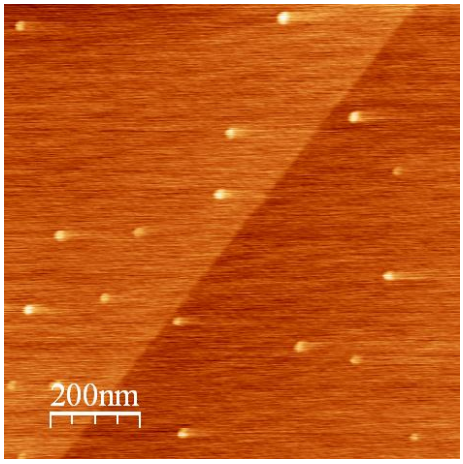

Fig. 1: Scanning force microscopy (SFM) topographic image of a CaF_2(111) surface irradiated by 3.1 keV/amu Xe^{40+} ions. Each impact produces one surface hillock with a volume of typically 200 nm^3.

The size of the hillocks is strongly correlated to the deposited potential energy. Estimations of the energy density deposited on the surface atoms indicated that the threshold can be linked to a solid-liquid phase transition [6]. The similarity between HCI and swift heavy ions is probably originating form the fact that in both cases the energy is initially depositied in the electronic subsystem of the solid leading to strong electronic excitations and ionizations.

Encouraged by these results and for getting a better understanding of the basic mechanisms concerning HCI induced modifications in ionic fluoride single crystals, we have started to study other alkaline-earth fluorides (BaF_2). Despite the same crystalline structure of both BaF_2 and CaF_2, we observed pronounced differences in the sensitivity to ion-induced surface damage. In order to reveal the damage created by HCI, we have used the technique of selective chemical etching.

Our preliminary results show that HCI impact creates etchable triangular-shaped pits in BaF_2, as shown in Fig. 2.

Investigations of BaF_2(111) surfaces after irradiation with various HCI of different charge states and kinetic energies is in progress.

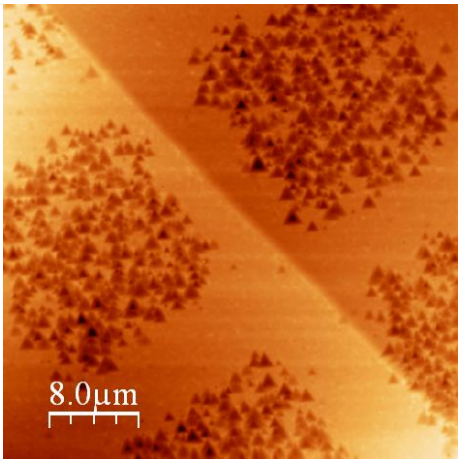

Fig. 2 SFM topographic image of a BaF_2(111) surface after chemical etching. The samples were irradiated with 0.7 keV/amu Xe^{19+} through a structured mask.

References: [1] Akcöltekin E. et al. *Nature Nanotechnology* **2** (2007) 290. [2] El-Said A.S. et al. *Nucl. Instrum. Meth. Phys. Res. B* **256** (2007) 313. [3] Aumayr F. et al. *Nucl. Instrum. Meth. Phys. Res. B* **266** (2008) 2729. [4] Heller R. et al. *Phys. Rev. Lett.* **101** (2008) 096102 (2008). [5] El-Said A.S. et al. *Nucl. Instrum. Meth. Phys. Res. B* **258** (2007) 167. [6] El-Said A.S. et al. *Phys. Rev. Lett.* **100** (2008) 237601.

DEGRADATION OF COVER SiO_2 ON Ge DURING Ga IMPLANTATION. J. Fiedler[1], V. Heera[1], L. Bischoff[1], S. Facsko[1], K.-H. Heinig[1], A. Mücklich[1], M. Posselt[1], H. Reuther[1], B. Schmidt[1], M. Voelskow[1], C. Wündisch[1] W. Skorupa[1] and G. Gobsch[2], [1]Forschungszentrum Dresden-Rossendorf, Institute of Ion Beam Physics and Materials Research, P.O. Box 51 01 19, 01314 Dresden, Germany, [2]TU Ilmenau, Institut für Physik, P.O. Box 10 05 65, 98684 Ilmenau, Germany

Introduction: Germanium is currently considered as a potential replacement for silicon [1]. The formation of heavily doped, shallow junctions in Ge by ion implantation and appropriate annealing techniques is under investigation [2,3]. In contrast to Si the Ge surface is severely affected by irradiation damage. Implantation into the uncovered Ge surface leads to surface roughening and even porous layers [3]. Therefore, the Ge surface must be protected by a thin cover layer, which is commonly a sputtered SiO_2-layer between 10 and 30 nm. This cover layer remains on the Ge sample also during annealing. For light dopants like B or P this oxide layer remains stable and smooth. However, with increasing ion mass and fluence surface erosion and oxide degradation can occur. A relatively heavy ion of interest is Ga [3], as shallow acceptor with a high solid solubility in Ge. We studied the effect of Ga implantation through a SiO_2 cover layer.

Experimental: Czochralski-grown n-Ge wafers of (100) orientation were used as substrates. Prior to processing the wafers were capped with 10 nm or 30 nm SiO_2 by sputter deposition. The wafers were implanted with a Ga fluence of $2x10^{16}$ cm^{-2} at an ion energy of 100 keV. The current density was about 0.5 µA/cm^2. Beam heating raises the target temperature (nominal room temperature) by about 50..150 K in dependence of the thermal contact to the sample holder. After implantation some samples were subjected to flash lamp annealing (FLA) or rapid thermal annealing (RTA) at temperatures between 500°C and 900°C. The surface structure was analyzed by scanning electron microscopy (SEM), atomic force microscopy (AFM) and Auger electron spectrometry (AES). Cross sections were prepared in order to investigate the layer morphology by transmission electron microscopy (XTEM).

Results: The 30 nm thick SiO_2 withstands both the Ga implantation and the subsequent annealing with only negligible surface erosion. As the XTEM analysis reveals less than 5 nm of the cover layer are lost by ion sputtering. However, ion beam mixing takes place at the Ge-SiO_2 interface, leading to Ge enrichment in the cover layer as well as to Si and O tails into the Ge substrate. After FLA at 900°C a δ-layer of nanocrystals consisting of Ge and/or Ga is formed in the SiO_2 layer as shown in Fig. 1. A certain analysis of the nanocrystals was not possible, because both Ga and Ge have very similar lattice spacings. The formation of Si nanocrystals in SiO_2 on Si after ion irradiation and annealing is known from literature [4].

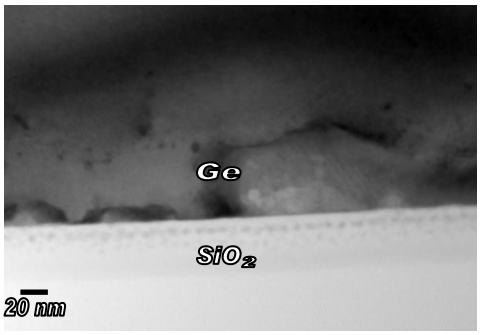

Fig. 1: XTEM micrograph showing a band of nanocrystals in the SiO_2 layer after Ga implantation and subsequent flash lamp annealing.

The application of thinner SiO_2 layers is much more problematic. Already in the as-implanted state the cover layer is partly (Fig. 2) or even completely eroded. As a consequence porous Ge has been formed. The origin of this effect and its inhomogeneity is not yet clear. It can be speculated that the Ge and/or Ga content in the cover layer enhances the low temperature dissociation of SiO_2. A further hypothetical mechanism is the melting of Ga-rich clusters. Ga melts at about 30°C and reduces the melting temperature of Si and Ge based phases.

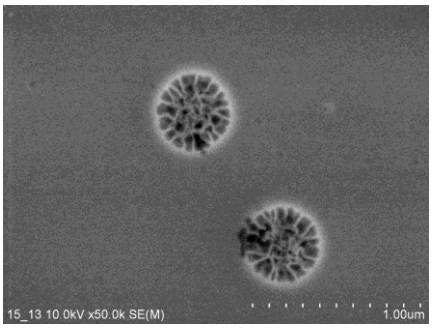

Fig. 2: SEM micrograph showing holes in the 10 nm thick SiO_2 surface with porous Ge at the bottom formed during implantation.

References: [1] Claeys C. and Simoen E. *Germanium-Based Technologies–From Materials to Devices* (Elsevier, New York, 2007). [2] Wündisch C. et al. *Appl. Phys. Lett.* **95** (2009) 252107. [3] Impellizzeri G. et al. *J. Appl. Phys*. **106** (2009) 013518. [4] Röntzsch L. et al. *Nucl. Instr. Meth. Phys. Res.* **B 242** (2006) 149.

ANNEALING OF SILICON NANOPATTERNS. M. Fritzsche[1], A. Keller[1], S. Facsko[1], K. Lenz[1] and J. Fassbender[1], [1]Institute of Ion Beam Physics and Materials Research, Forschungszentrum Dresden-Rossendorf, 01328 Dresden, Germany

The morphology of surfaces strongly influences optical, electrical, and magnetic properties of thin films. By changing the morphology it is possible to tailor the material properties. Oblique low energy ion beam sputtering produces periodic ripple structures with periodicities in the nanometer range. During sputtering the region near to the surface gets amorphous and some metal is deposited on the surface, i.e. Cu from the sample holder. These ripple patterns can be used as templates. By using amorphous ripples only polycrystalline films can be grown. These films have a morphology induced dipolar anisotropy. In order to grow the films epitaxially the ripples have to be crystalline. Hence, this could induce an additional anisotropy in a magnetic overlayer. One possible route to achieve crystalline ripples is annealing. Therefore, the annealing temperature dependence was studied using STM. With increasing temperature the ripples vanish. They are not removed by a reduction of the amplitude, but by the creation of circular voids. Inside these voids the surface exhibits few steps and is otherwise flat on an atomic scale. In the middle of the voids Cu clusters are found, which appear at steps. Inside the crystalline area of the voids the Si(111) "quasi 5×5" Cu surface is found. For larger temperatures the number and size of these voids increases until the ripples are removed from the whole surface.

ION TRACK LITHOGRAPHY. H.-G. Gehrke[1], A.-K. Nix[1], J. Krauser[2], C. Trautmann[3], A. Weidinger[4], U. Vetter[1], H. Hofsäss[1], [1]II. Physikalisches Institut, Universität Göttingen, Germany, [2]Hochschule Harz, Wernigerode, Germany, [3]Gesellschaft für Schwerionenforschung, Darmstadt, Germany, [4]Hahn-Meitner-Institut, Berlin, Germany

Swift Heavy ions create latent tracks in polycarbonate. Chemical wet etching allows selective removal of the polymer along the ion path creating small pores through the film.

We developed a method to create thin polycarbonate films by spin coating, allowing the etching of pores with diameters in the range of 50 – 80 nm. These pores can be used as templates to structure the substrate. Depositing materials (e.g. gold) through the pore results in clusters on the substrate. Sputtering through the pores in the polymer mask creates holes in the substrate. Combining both procedures produces buried clusters, which might be favorable to grow nano wires on top. In addition, the creation of electrode structures is possible by combining the single ion lithographic process with conducting ion tracks in tetrahedral amorphous carbon (ta-C). We demonstrate the principle of creating such a structure using the self-alignment of the ion tracks.

COMPARISON OF CONVENTIONAL AND HIGH-RESOLUTION ERD. M. Kosmata, D. Hanf, F. Munnik, M. Vieluf, W. Möller, Institute of Ion Beam Physics and Materials Research, Forschungszentrum Dresden-Rossendorf, P.O. Box 510119, 01314 Dresden, Germany, m.kosmata@fzd.de

Introduction: Nowadays there are many fields of highly innovative technologies that benefit strongly from the application of surface analysis techniques in research, manufacturing and quality control. The quantitative elemental analysis of layers and layer sequences in the thickness range of a few nanometres has become of rising technological relevance in recent years. The focus of these materials science issues is the determination of the depth distribution of elements in thin layers, which are achieved by sequential deposition processes or subsequent process steps such as annealing, but also the detection of unintended contamination. This information is very useful for materials development and for the validation of existing process control functions.

ERD: Elastic Recoil Detection (ERD) is an analytical technique in materials science to obtain concentration depth profiles for light elements in thin films. For these measurements heavy ions from the FZD 5-MV-Tandem accelerator are directed to the sample. The ejected recoil atoms are detected and analysed by their energy under forward direction. The depth resolution directly correlates with the energy resolution of the detector. The depth scale is provided by the stopping power of energetic heavy ions interacting with matter.

HR-ERD @ FZD: High energy resolutions can be obtained using magnetic particle spectrometers, where energy information is transformed into position information. The magnetic spectrometer for elemental analysis with high depth resolution at FZD, the QQDS magnetic spectrometer, is named "Little John" (Fig. 1). It consists of a dipole to separate particles according to their momentum and two quadrupoles and one sextupole to focus the recoil atoms on the detector plane.

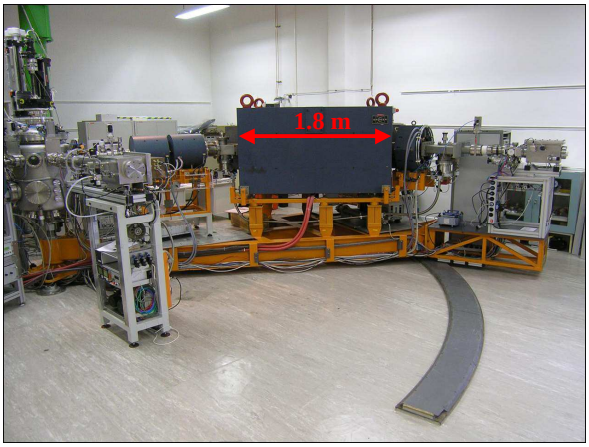

Fig. 1: QQDS magnetic spectrometer "Little John".

Comparing ERD & HR-ERD: To demonstrate the excellent performance of the new high-resolution ERD set-up at FZD, we investigated the performance for quantitative depth profiling and surface analysis in direct comparison to our of conventional ERD set-up. Advantages and limits for both techniques have been clearly identified: E.g. spectroscopy of recoil ions and scattered projectiles in a single measurement is an important convenience of conventional ERD. Whereas its near-surface depth resolution - even under optimised conditions - is about ten times worse (~10 nm) than those of HR-ERD (~1 nm) (Fig. 2). One disadvantage of magnetic spectrometers is that particles with identical momentum but different charge state are also separated. So it is absolutely necessary to measure the depth-depended charge state distribution (as shown e.g. in [1]). In addition, such a measurement yields results fro only one element. Therefore, conventional ERD might be needed to obtain global information about the sample. Furthermore, additional analysing techniques, like atomic force microscopy, are needed as the sample topography is strongly influencing the quality of quantification procedures.

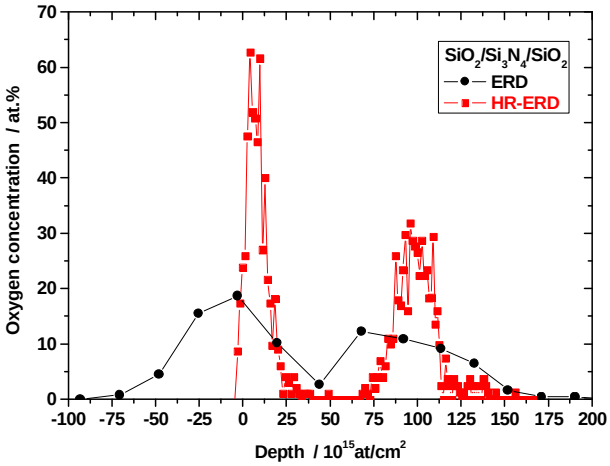

Fig. 2: Oxygen concentration of a SiO_2-multilayer measured by ERD and HR-ERD, respectively.

References: [1] Wiemann R. et al. *this meeting*.

TAILORING THE MAGNETISM OF GaMnAs BY ION IRRADIATION. Lin Li[1,2], Shengqiang Zhou[2], Danilo Bürger[2], Olga Roshchupkina[2], Andrew Rushforth[3], R.P.Campion[3], Shude Yao[1], J. Grenzer[2], Jürgen Fassbender[2], Manfred Helm[2], Bryan Gallagher[3], Carsten Timm[4], Heidemarie Schmidt[2], [1]State Key Laboratory of Nuclear Physics and Technology, Peking University, Beijing 100871, China, l.li@fzd.de, [2]Institute for Ion Beam Physics and Materials Research, Forschungszentrum Dresden- Rossendorf., Bautzner Landstraße 400, 01328 Dresden, Germany, [3]School of Physics and Astronomy, University of Nottingham, Nottingham NG7 2RD, United Kingdom, [4]Institute for Theoretical Physics, Technische Universität Dresden, 01062 Dresden, Germany

Introduction: The properties of magnetic metals such as saturation magnetization and magnetic anisotropy can be modified in a controllable manner by energetic ions [1]. GaMnAs is a well-known magnetic semiconductor. The ability to tune the magnetic properties of magnetic semiconductors is an important issue in future semiconductor devices. Using low temperature annealing it has been shown that the micromagnetic structure of GaMnAs may be influenced in a controlled manner [2]. Here we tailored the magnetism of GaMnAs films by He^+ ion irradiation. The $Ga_xMn_{1-x}As$ films with a Mn concentration of 5% and the easy axis of magnetization lying in-plane have been grown on GaAs substrates by low temperature molecular beam epitaxy (LT-MBE). He^+ ions of 650 keV were used to place the peak of damage into the GaAs substrate, so that the GaMnAs epilayer lies in the relatively uniform part of the damage profile. We show that the coercivity can be increased (Fig. 1) from 50 Oe to 165 Oe when the He^+ ion dose reaches $3\times10^{14}/cm^2 \sim 6\times10^{14}/cm^2$. Meanwhile, the saturation magnetization at 5 K is only reduced slightly to 22 emu/cm^3 compared to non-irradiated GaMnAs films with a saturation magnetization amounting to 27 emu/cm^3. Magneto-transport results indicate that the sheet resistance is increased by about 4 times compared to the non-irradiated GaMnAs film with a sheet resistance of 10^3 Ω. The irradiated GaMnAs still has an in-plane easy axis of magnetization at 5 K, but the anisotropy energy is much decreased. When the dose increases to $1\times10^{15}/cm^2$ (black solid line in Fig. 1), no M-H hysteresis has been probed. Our study demonstrates the tailoring of magnetism and magnetoresistance in GaMnAs films by He^+ ion irradiation.

Digital Formats: Fig. 1 M-H hysteresis loop probed at 5 K on different GaMnAs films. After He^+ ion irradiation, the coercivity increases strongly and the saturation magnetization decreases slowly. When the He^+ ion dose reaches $3\times10^{14}/cm^2 \sim 6\times10^{14}/cm^2$, the coercivity is increased by more than three times, while the saturation magnetization reduces slightly: less than 1/5. When the dose increases to $1\times10^{15}/cm^2$, magnetism diminishes.

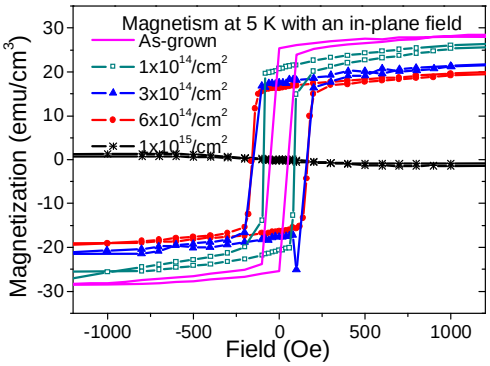

References: [1] Fassbender J. and McCord J. *J. Magn. Magn. Mater.* **320** (2008) 579–596. [2] Pross A., Bending S., Edmonds K., Campion R.P., Foxon C.T. and Gallagher B. *J. Appl. Phys.* **95** (2004) 3225-3227.

ION INDUCED SURFACE PATTERN EVOLUTION DESCRIBED BY COMBINED TRIM AND KINETIC MONTE-CARLO SIMULATIONS. B. Liedke, K. H. Heinig, S. Facsko, W. Möller, Institute of Ion Beam Physics and Materials Research, Forschungszentrum Dresden-Rossendorf, Dresden, Germany

Atomistic understanding of surface morphology evolution induced by ion beam sputtering is still strongly limited. Available continuum models cannot explain microscopic processes during ion beam irradiation. On the other hand, so far atomistic simulations could not describe pattern dynamics in the spatiotemporal scales of experiments.

However, combined atomistic single ion impacts with continuum equations [1] gives a better understanding of additional smoothing mechanisms, like an effective mass 'downhill' current induced by ballistic atomic drift [2,3].

We developed a novel program package which unifies the collision cascade with kinetic Monte-Carlo simulations. The 3D atom relocations were calculated in the Binary Collision Approximation (BCA), whereas the thermally activated relaxation of energetic atomic configurations as well as diffusive processes were simulated by a very efficient bit-coded kinetic 3D Monte Carlo code.

Effects like ballistic mass drift or dependence of local morphology on sputtering yield are automatically included in the BCA approach. Distributions presented in Figure 1 show the mean preferential location of ad-atoms creation and the sputtering regions.

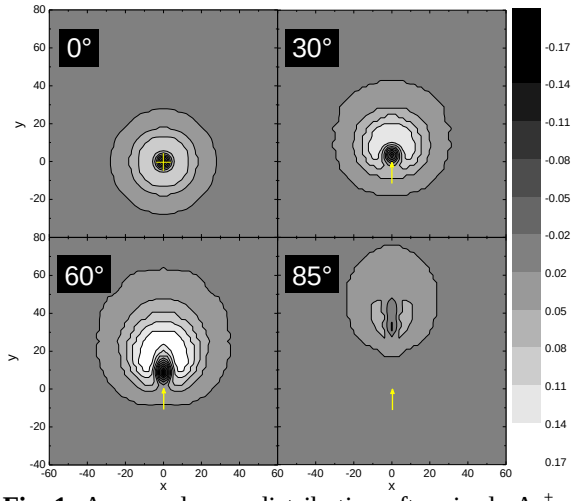

Fig. 1: Averaged mass distribution after single Ar^+ ion impacts at 1 keV onto Si target.

Low energy (up to 5 keV) ion sputtering simulations have been performed on the simulation cell of about 17 million atoms, where irradiation fluence goes up to few 10^{18} cm^{-2}. The pattern topography has been study by means of various intensive parameters like incidence angle (Fig. 2), ion beam energy, ion fluence, and migration energy of defects. Moreover, the scaling behaviour of surface roughness and pattern periodicity has been analysed.

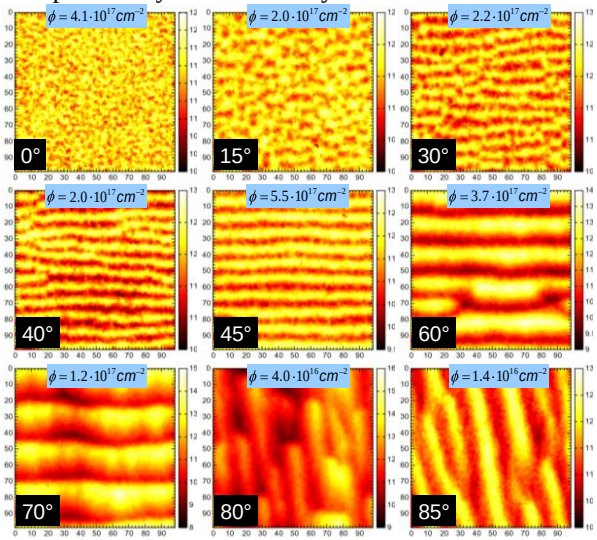

Fig. 2: Simulated surface pattern after 0.8-1 keV Ar^+ irradiation of (001)Si for different ion fluences and incidence angles. KMC with $\varepsilon_{NN}/k_BT=1.7$.

Finally, we compare our results with experiments as well as with continuum theory.

References: [1] Norris S.A., Brenner M.P. and Aziz M.J. *J. Phys. Condens. Matter* **21** (2009) 224017. [2] Carter G. and Vishnyakov V. *PRB* **54** (1996) 17647. [3] Moseler M., Gumbsch P., Casiraghi C., Ferrari A.C. and Robertson J. *Science* **309** (2005) 1545.

DOUBLE SPIN REORIENTATION TRANSITION IN Pt/Co/Pt FILMS AFTER Ga ION IRRADIATION.

P. Mazalski[1], A. Maziewski[1], M. Tekielak[1], J. Ferré[2], J. Jaworowicz[1,2], A. Mougin[2], B. Liedke[3], M.O. Liedke[3], J. Fassbender[3], [1]Department of Physics, University of Bialystok, ul. Lipowa 41, Bialystok, Poland, piotrmaz@uwb.edu.pl, magnet@uwb.edu.pl, tekmar@uwb.edu.pl, jawor@uwb.edu.pl, [2]Laboratoire de Physique des Solides, UMR CNRS 8502, Université Paris-Sud, 91405, Orsay, France, mougin@lps.u-psud.fr, ferre@lps.u-psud.fr, [3]Institute of Ion Beam Physics and Materials Research, Forschungszentrum Dresden-Rossendorf, Dresden, Germany, b.liedke@fzd.de, m.liedke@fzd.de, j.fassbender@fzd.de

Ion irradiation is known as an elegant tool to tune the magnetic properties of ultrathin films, in which the perpendicular anisotropy is mainly of interfacial origin [1,2]. In previous studies light He ions were used to tune the magnetic properties of Pt/Co/Pt films with an initial out of plane magnetization. Upon irradiation Co and Pt ions intermix at interfaces so that the resulting disorder leads to a reduction of magnetic anisotropy, coercive field and Curie temperature. Increasing the He ion dose, a spin reorientation transition (SRT) to in-plane has been evidenced. With much efficient heavier ions, like Ga, a similar SRT occurs, but at a lower dose [3]. How-ever, we reported recently on the discovery of an opposite in-plane to out-of-plane SRT under very low Ga ion dose in thicker Co films [4]. Ga ion irradiation is especially appealing since these ions are used in state of the art Focused Ion Beam (FIB) systems, that enables patterning with resolution below 10 nm.

Here we report on an extension of our previous work [4]. High quality Pt(4.5 nm) / Co(2.6 nm) / Pt(3.5 nm) films were sputter deposited on a sapphire substrate. The virgin film exhibiting in-plane magnetic anisotropy was irradiated through 1mm wide strip regions by 30 keV Ga ions with different doses D ranging from $2x10^{13}$ to $7x10^{14}$ Ga ions/cm^2. These regions were studied using both, magnetometry and imaging techniques: (i) polar Kerr PMOKE milli-magnetometry with a red light spot with 0.4 mm size (to check the out-of-plane magnetization component, with the possibility of applying a magnetic field at different, polar -θH- and azimuthal -φH- angles); (ii) optical microscopy enabling high spatial resolution studies of out-of-plane or in-plane magnetized domains using polar or longitudinal magneto-optical Kerr effects (PMOKE or LMOKE). Moreover, magnetic force microscopy (MFM) was used to image small size domain patterns. TRIDYN simulations were performed to study irradiation driven ion distributions.

Figure 1A shows polar hysteresis loops for increasing doses. For 1 and $2x10^{14}$ Ga ions/cm^2 the square and remnant hysteresis loops demonstrate that the magnetic anisotropy is out-of-plane. This is confirmed by the submicrometer magnetic domain structure, visualized by MFM (Figure 1B). The domain structure is similar to the one observed in an as-deposited ultrathin Co film with a thickness below the SRT [4,5]. Increasing further the ion dose, the magnetization drops again towards the film plane. So, at the early stage of irradiation, an unexpected SRT from an in-plane magnetization state towards an out-of-plane one was observed. Higher ion doses D induce a second inverse SRT from an out-of-plane state into an in-plane one. So Ga irradiation induces a double SRT in Pt/Co(2.6 nm)/Pt films. Nevertheless, the origin of this behavior differs from that evidenced in Cu/Ni/Cu films when increasing the Ni layer thickness [6].

These results will be discussed considering an irradiation induced alloying process in Co and Pt layers. Figure 2 shows the ion distributions determined for an irradiated film with out of plane magnetization.

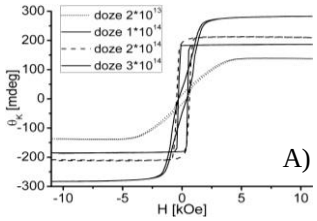

Fig.1: A) Hysteresis loops measured in P-MOKE configuration for various Ga ion dose. B) MFM image (10x10 μm^2) of the magnetic domain structure in the Ga irradiated zone with D = $1x10^{14}$ ions/cm^2.

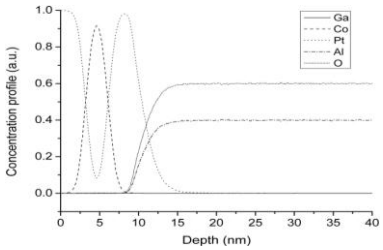

Fig.2: In-depth ion distributions determined from TRIDYN for D = $1.5x10^{14}$ ions/cm^2 (solid vertical lines correspond to the initial position of Pt/Co and Co/Pt interfaces, respectively).

References: [1] Ferré J. and Jamet J.-P. in *Handbook on Magnetism and Advanced Materials* (Eds. Kronmüller H. and Parkin S.) **3** (2007) 1710. [2] Fassbender J. and McCord J. *J. Magn. Magn. Mat.* **320** (2008) 579. [3] Vieu C. et al. *J. Appl. Phys.* **91** (2002) 3103. [4] Jaworowicz J. et al. *Appl. Phys .Lett.* **95** (2009) 022502. [5] Kisielewski M. et al. *JMMM* 260 (2003) 231. [6] Bochi G. et al. *Phys. Rev. B* **53** (1996) R1729.

This work was partly supported by the EU-"Research Infrastructures Transnational Access" program "Center for Application of Ion Beams in Materials Research" under contract no. 025646 and DAAD.

CARBONATE MINERALS AND SWIFT HEAVY ION IRRADIATION. S. Pabst[1], M. Burchard[1], U.A. Glasmacher[1], S. Dedera[1], R. Miletich[1], B. Schuster[2], C. Trautmann[2], R. Neumann[2], [1]Institut für Geowissenschaften, Im Neuenheimer Feld 234, 69120 Heidelberg, Germany, sonja.pabst@geow.uni-heidelberg.de, [2]GSI Helmholtzzentrum für Schwerionenforschung, Planckstraße 1, 64291 Darmstadt, Germany

Introduction: Carbonate minerals such as calcite ($CaCO_3$), aragonite ($CaCO_3$), and dolomite ($CaMg(CO_3)_2$) build up large rock masses on Earth. The dissolution of such carbonate minerals is important for understanding the impact of climate change on Earth surface and water chemistry. The occurrence of crystallographic defects influences the dissolution rate of these carbonate minerals. Given the fact that carbonate minerals can incorporate uranium as a trace element during their growth, the material may be damaged due to fission tracks by natural decay of uranium. Spontaneous fission tracks in carbonate minerals can be suitable for application as new low-temperature thermochronometer. The development of a new dating tool requires a detailed understanding of the behavior of fission tracks at natural pressure and temperature conditions. We therefore use swift heavy ion irradiations to simulate defect creation of fission tracks in variable amount, size and shape. Therefore, calcite, aragonite and dolomite were irradiated with ^{238}U of 11.1 MeV/u energy at fluences between 10^6 and 10^{12} ions/cm^2. In addition, calcite mounted within the new Paris-Edinburgh press (applied pressure 2.9 GPa) was irradiated using U ions (10^{12} cm^{-2}) of 400 MeV/u initial energy.

Results: Raman spectra of pristine and ^{238}U ion irradiated calcite in the fluence range of up to 10^{12} ions/cm^2 are shown in Fig. 1a. Irradiating calcite with increasing fluence at ambient pressure causes defects that produce changes in the micro-Raman spectra. Compared to the non-irradiated sample, the peak positions do not change but the intensity of the major bands decreases [compared to 1] and the band widths slightly increase. Due to broadening, the small band at 1066 cm^{-1} finally merges with the strongest band at 1086 cm^{-1}. At a fluence of 10^{11} ions/cm^2, a new band appears at 429.5 cm^{-1}, at a fluence of 10^{12} ions/cm^2 additional bands appear at 1385 cm^{-1} and 1707 cm^{-1}.

The irradiation under pressure also influences the micro-Raman spectra of calcite (Fig. 1b): the overall intensity decreases by a factor of 10 due to mechanical deformation, and new Raman bands appear at 429.5 cm^{-1} (due to the irradiation with 10^{12} ions/cm^2) and at 490 cm^{-1}. The band at 1066 cm^{-1} disappears under high pressure. Peak positions do not change, but the half width of the bands increases.

Irradiation of calcite with swift heavy ions causes an increasing number of defects likely accompanied by the formation of new phases. Possible CO_2-loss should form CaO phases. Further investigation is needed to understand how the calcite structure changes under ion irradiation.

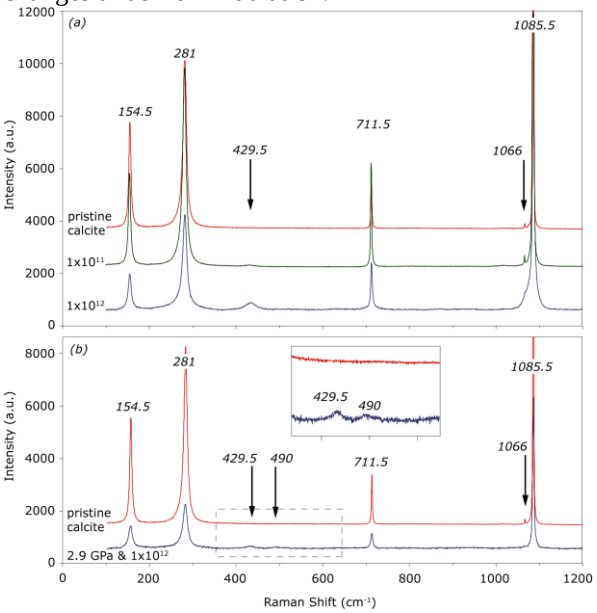

Fig. 1: Raman spectra (baseline corrected) of pristine, irradiated, and pressurized calcite. (a) Samples irradiated with ^{238}U of 11.1 MeV/u initial energy at a fluence of up to 10^{12} ions/cm^2 and b) pristine calcite compared to calcite at a pressure of 2.9 Gpa (10^{12} ions/cm^2 fluence).

References: [1] Nagabhushana S.C. et al. *Spectrochim. Acta A* **71** (2008) 1070-7073.

ERDA AND RBS MEASUREMENTS OF ORDERED FIBER STRUCTURE USING MACRO BEAM.

V. Peřina, P. Malinský and R. Mikšová, Nuclear Physics Institute of Academy Sciences of Czech Republic, v.v.i., Řež near Prague CZ 250 68, Czech Republi,c perina@ujf.cas.cz

Introduction: Lately, carbon nanotubes and fibers are widely used and studied due their interesting physical and chemical properties. Their applications lay in field of catalysis, electronic, medicine, analytical tools, and adsorption and as a frame for polymer filling. Many physical and chemical methods such as STM, TEM, neutron diffraction, XRD, XPS, XRF, ICP AES, TEM, EELS infrared and Raman spectroscopy are usually applied for analyzing their chemical and structural composition. N and S are quantified by combustion in oxygen and by conductivity measurements [1-3]. The drawback of most mentioned methods is either bulk or surface sensitivity. Nuclear analytical methods ERDA and RBS can overcome this problem, but the big problem is roughness of nanotubes or fibers systems. We chose oriented fibers systems as an attempt of estimation of oxygen and hydrogen contend in depth profiles. Lately some experimental and theoretical studies were published [4-8]. The roughness effect is essential for grazing angles. The thickness inhomogeneity leads to different energy losses in different layer positions and the corresponding signal is propagated to lesser energy i.e. to the position of deeper layer. The small roughness leads to additional Gaussian broadening contribution comparable with FWHM of detector resolution.

Experimental: We measured oriented carbon fiber system in three various geometries: Parallel, perpendicular and 45° to plane beam – detector. As can be seen in Fig. 1, there are big differences in ERDA spectra. The geometry was as follows: Incident angle 75°, exit angle 75°, scattering angle 30°. Conventional ERDA with incident 2.7 MeV alpha particles and detector covered 10 μm thick foil was used. For the parallel geometry the spectrum is very analogous to that for a flat sample, with only slight signal propagation to lesser energy i.e. to the position of deeper layer and with strong surface signal. For other geometries the substantial part of surface signal is shifted to lower energies. The schematic drawing in Fig. 2 shows the uttermost path of impinging and scattered ion beams. The RBS spectra for oxygen estimation on the contrary lead to slight highlighting of oxygen surface signal. It can be explained by only very thin surface oxide layer.

Conclusion: The parallel arrangement of carbon fibers was used for ERDA and RBS measurements in various sample directions and differences in spectra shape was used for bulk or surface admixture estimation.

References: [1] Maldonadoa S., Morina S. and Stevenson K.J. *Carbon* **44** (2006) 1429-1437. [2] Belin T. and Epron F. *Materials Science and Engineering B* **119** (2005) 105-118. [3] Tessonnier J.-P., Rosenthal D., Hansen T.W., Hess C., Schuster M.E., Blumea R., Girgsdiesa F., Pfänder N., Timpe O., Su D.S. and Schlögl R. *Carbon* **47** (2009) 1779-1798. [4] M. Mayer *NIM* **B194**, (2002), 177-186. [5] Barradas N., Alves E., Pereira S., Shvartsman V.V., Kholkin A.L., Pereira E., O`Donnell K.P., Liu C., Deather C.J., Watson I.M. and Mayer M. *NIMB* **217** (2004) 479-497. [6] Mayer M., Fischer R., Linding S., von Toussaint U., Stark R.W. and Dose V. *NIM B* **228** (2005) 349-359. [7] Marin N, Serruys Y. and Calmon P. NIM B **108** (1995) 179-187. [8] da Silva A.A. and Tabacniks M.H. *Publicacao IF* -**146**/2000, Instituto de Fisica, Univ. Sao Paulo.

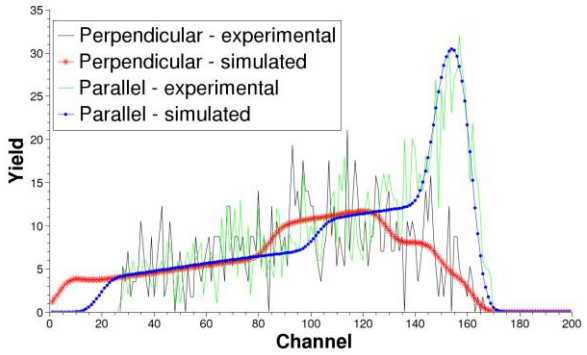

Fig. 1: ERDA spectra for perpendicular and parallel geometry.

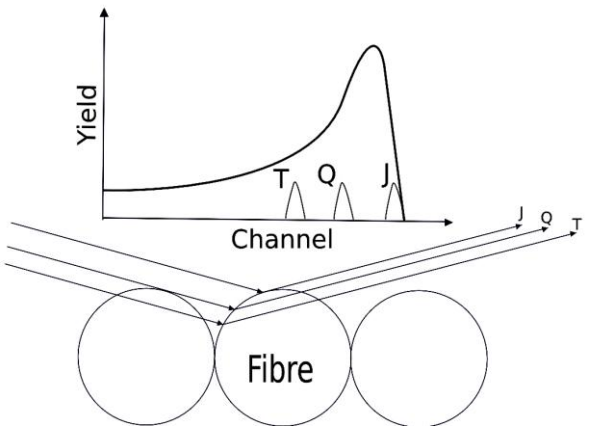

Fig. 2: Schematical measuring geometry.

OPTICAL AND MICROSTRUCTURAL PROPERTIES OF InAs QUANTUM STRUCTURE MADE BY ION IMPLANTATION AND FLASH LAMP PROCESSING. S. Prucnal, A. Shalimov, A. Kanjilal, S. Zhou and W. Skorupa, Institute of Ion Beam Physics and Materials Research, Forschungszentrum Dresden-Rossendorf, P.O. Box 510119, 01314 Dresden, Germany, s.prucnal@fzd.de, a.shalimov@fzd.de, a.kanjilal@fzd.de, s.zhou@fzd.de, w.skorupa@fzd.de

Introduction: The InAs quantum structures were formed in silicon by sequential ion implantation and subsequent thermal annealing. Samples were characterized by μ-Raman spectroscopy, Rutherford Backscattering Spectrometry (RBS), low temperature photoluminescence (PL), high resolution transmission electron microscopy (HRTEM) and X-ray diffraction (XRD). Two kinds of crystalline InAs nanostructures were successfully synthesized: quantum dots (QDs) and nanopyramides (NPs). The Raman spectrum shows two peaks at 215 and 235 cm^{-1} corresponding to the transverse optical (TO) and longitudinal optical (LO) InAs phonon modes, respectively. The narrow PL band at around 1.3 μm from the InAs QDs with an average diameter (7.5 ± 0.5) nm was observed.

The InAs NPs were found only in samples annealed for 20 ms at temperature range from 1000 up to 1200°C. The crystallinity and pyramidal shape of InAs quantum structures were confirmed by high resolution transmission electron microscopy (HRTEM) (see Fig. 1) and X-ray diffraction (XRD). The average size of the NPs is 50 nm base and 50 nm high and they are oriented parallel to the Si(001) planes. The InAs nanopyramids grow in silicon due to liquid phase epitaxy.

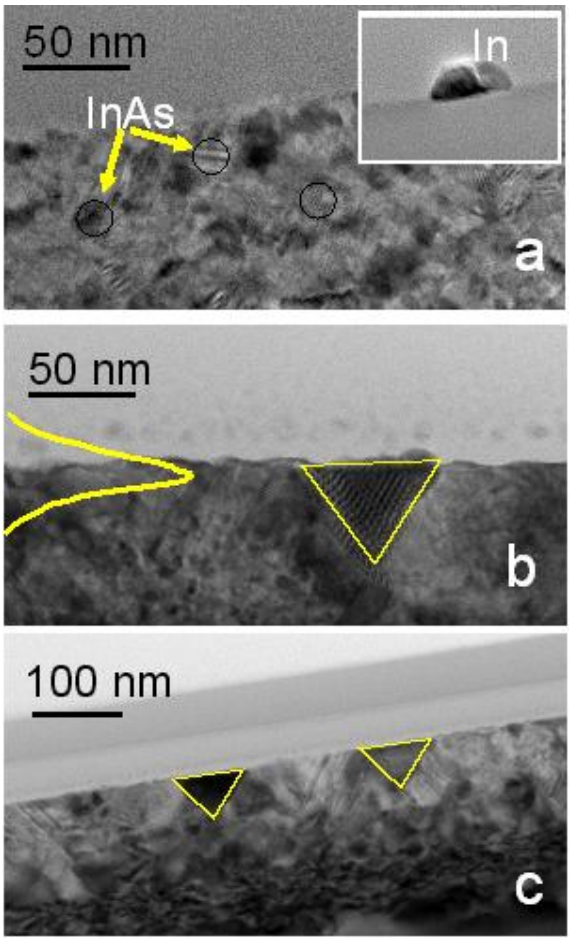

Fig.1: Bright field HRTEM micrographs of Si coimplanted by As and In followed by annealing at 850°C for 1 min (a), 1150°C for 20 ms (b) and 1200°C for 20 ms (c). Inset of figure 1a shows In nanopyramids formed on the SiO_2 surface. The yellow line in Fig 1b shows the RBS profile of In and As.

SELF-ORGANISATION OF METAL NANOPARTICLES ON ION BEAM PRODUCED RIPPLE TEMPLATES. M. Ranjan*, S. Facsko ,W. Möller, Institute of Ion Beam Physics and Materials Research, Forschungszentrum Dresden-Rossendorf, Bautzner Landstrasse 400, 01328 Dresden, Germany, m.ranjan@fzd.de

Introduction: Ion beam sputtering has been used for pre-structuring of the substrate. Low energy ion beam (Ar^+, 500 eV) incident on the substrate surface (Si in our case) at an angle of 67° to the surface normal to produce well ordered (20-50 nm) ripple patterns [1,2]. The periodicity and regularity of the pattern is established by the effective filtering of a narrow band of spatial frequencies on the surface, which results from the interplay between a surface instability caused by the sputtering and surface diffusion processes. Regular ripple morphologies have been produced in this way on very different materials including semiconductors, isolators, and metals, demonstrating the universality of the mechanism [2].

Depending on deposition angle, substrate temperature, beam flux, and deposition time, the metal nanostructures align parallel to the ripples, eventually coalesce forming nanowires [3,4]. A very high degree of alignment not reported so far using the present technique has been achieved. Due to the alignment the nanoparticles exhibit strongly anisotropic optical properties. The difference in the interparticle distance along the parallel and perpendicular direction, respectively, leads to different plasmonic coupling in the respective directions. Therefore a red shift of the plasmon-polariton resonance is observed for light polarized parallel to the ripple direction. In addition, the resonance shifts with the aspect ratio of the nanoparticles. Energy shifts of the plasmon resonance of 0.2 eV to 0.7 eV have been determined for aspect ratios in the range of 2 to 5.

References: [1] Keller A., Rossbach S., Facsko S. *Nanotechnology* **19** (2008) 135303. [2]. Keller A., Facsko S., Möller.W. *Jour. Phys. Cond. Matt.* **21** (2009) 495305. [3] Oates T.W.H., Keller A., Facsko S., Mücklich A. *Plasmonics* **2** (2007) 47. [4] Oates T.W.H., Keller A., Noda S., Facsko S. *Appl. Phys. Lett.* **93** (2008) 063106.

SELF-ORGANIZATION OF Fe-Pt NANOPARTICLES IN MgO AFTER SEQUENTIONAL ION IMPLANTATION AND HIGH-TEMPERATURE ANNEALING. A. Shalimov, S. Zhou, N. Jeutter and K. Potzger, Forschungszentrum Dresden-Rossendorf, Institute of Ion Beam Physics and Materials Research, Bautzner Landstr. 400, 01328 Dresden, Germany (e-mail: a.shalimov@fzd.de)

In the present study we report structural and magnetic properties of FePt nanoparticles synthesized by ion implantation and post-implantation high temperature annealing. Conditions of $Pt^+$and Fe^+ ion implantation and high-temperature annealing have been optimized in the aim of synthesis of magnetic FePt nanoparticles in magnesium oxide. We demonstrate that self-organization of FePt nanoparticles occurs exclusively at certain fluences of implanted ions and temperature conditions essential for the ions agglomeration. MgO single crystals were implanted with Fe and Pt ions using the equal fluences varied in the range from 1×10^{16} up to 1×10^{17} cm^{-2}. Energies of 180 keV for Fe ions and 530 keV for Pt ions were selected in order to overlap both ion distribution profiles at the depth of about 100 nm below the substrate surface. After the implantation, samples were annealed in high-vacuum chamber at different temperatures varying the annealing time. Samples characterization was performed by means of synchrotron radiation X-ray diffraction (SRXRD), Rutherford backscattering spectrometry (RBS), superconducting quantum interference device (SQUID) magnetometry and theoretical simulation of magnetic structure using the Preisach formalism. It was found that the MgO crystals implanted with 6×10^{16} cm^{-2} of Fe and Pt ions annealed at 800°C during 1 hour represent the highest coercive field and magnetic moment of FePt nanoparticles. The implantation of MgO with higher fluences of Fe^+ and Pt^+ is inappropriate for nanoparticles synthesis, since high ion fluences lead to creation of buried FePt layer. The influence of Pt ion beam current on the nanoparticles generation is additionally examined.

This work is performed within the framework of DFG Project PO 1275/2-1 “SEMAN”.

HYBRID MAGNETIC MATERIALS CREATED BY LOCAL ION IRRADIATION. T. Strache[1], O. Roshchupkina[1], M. Fritzsche[1], M.A. Basith[2], J. McCord[3] and J. Fassbender[1], [1]Forschungszentrum Dresden-Rossendorf, Germany, [2]University of Glasgow, UK, [3]Leibniz-Institut für Festkörper- und Werkstoffforschung Dresden, Germany

Lateral patterning of thin ferromagnetic films allows the modification of the magnetic parameters below certain intrinsic magnetic length scales like the domain wall width. In contrast to the creation of isolated micro- and nanostructures, magnetic patterning by means of local ion irradiation results in direct exchanged coupled regions in the thin film, which have different magnetic properties. At the lateral interfaces of these regions magnetic domain walls can be trapped and thus easily investigated. The modification of the material properties, e.g. saturation magnetization and magnetic anisotropy, also directly affects the intrinsic length scales.

As a model system periodic patterns of $Ni_{80}Fe_{20}$ stripes with alternating saturation magnetization value located either inside a $Ni_{80}Fe_{20}$ matrix or isolated are used. During the magnetic reversal with the external field parallel to the stripes, magnetic domain walls are created between adjacent stripes due to a none-parallel alignment of the stripe's magnetization (Fig. 1).

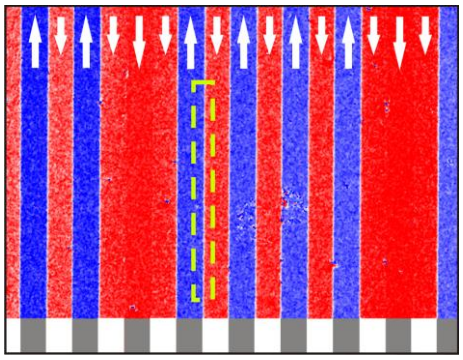

Fig. 1: Magnetization distribution in periodic pattern of 10 µm wide stripes with alternating saturation magnetization value. The magnetization directions are indicated by arrows. (Non-) irradiated regions with (unchanged) decreased saturation magnetization are indicated with (gray) white shaded areas at the bottom. The location of a 180° domain wall is indicated by the green rectangle.

As the wall profile for stripe widths in the sub-µm regime is not easily accessible in experiment, changes of the possible orientations of the magnetization inside the stripes with respect to the stripe orientation are used to obtain informations about the domain walls. For special pattern configurations these domain walls are able to mediate an exchange spring behavior through the storage of energy [1]. By scaling the stripes width down, a crossing between the patterning size and the intrinsic length scales associated with the domain walls is expected. This is combined with a transformation to an effective magnetic medium, showing neither the properties of the fully irradiated nor the unirradiated material (so-called hybrid material).

Local ion irradiation is accomplished by irradiation in combination with a lithographically defined mask or the by the use of a focused ion beam. For comparision the ion energies for both methods are choosen to be 30 keV. For a $Ni_{80}Fe_{20}$ film thickness of 20 nm the resulting penetration depths of the ions cover the complete film as well as the interface to the seed layer. In order to understand the ion irradiation induced changes in the magnetic parameters of the film, ions of different species (Ar^+, Ga^+, Cr^+, Ni^+, Co^+, Si^+, O^+) as well as different seed layers are used. Changes of the magnetic and structural properties are studied as function of ion species, fluence and seed layer material. The uniaxial magnetic anisotropy of the $Ni_{80}Fe_{20}$ film is not affected by the implanted ion species, but by the species of the recoils originating from the seed layer. Using SiO_2 as seed layer material, the anisotropy can be successively annihilated with increasing fluence. Irradiation using a Ga^+ focused ion beam with its high current density induces a grain growth to the material [2], limiting therefore also the minimum patterning size (Fig. 2).

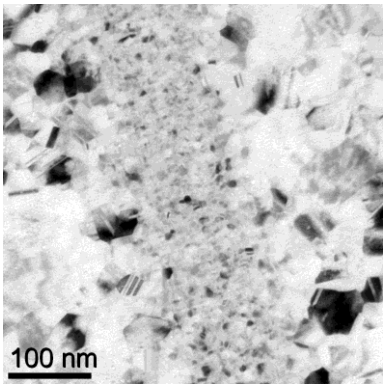

Fig. 2: Bright field plane view TEM image of 200 nm wide stripes. The focused ion beam irradiated areas are observable by the increased grain size.

References: [1] McCord J. et al. *Advanced Materials* **20** (2008) 2090. [2] Ozkaya D.L. et al. *Journal of Applied Physics* **91** (2002) 9937.

MEASUREMENT OF THE HYDROGEN CONCENTRATION IN INDIUM OXIDE TABULAR NOSTRUCTURES. M. Voelskow[1], D. Grambole[1], W. Skorupa[1], A. Kanjilal[1], M. Kumar[2], R. Chatterjee[2], S. Milikisiyants[3], K.V. Lakshmi[3] and J.P. Singh[2], [1]Institute of Ion Beam Physics and Materials Research, Forschungszentrum Dresden-Rossendorf, P.O. Box 510119, 01314 Dresden, Germany, e-mail: m.voelskow@fzd.de, [2]Department of Physics, Indian Institute of Technology Delhi, Hauz Khas, New Delhi-110016, India, [3]Department of Chemistry and Chemical Biology and The Baruch '60 Center for Biochemical Solar Energy Research, Rensselaer Polytechnic Institute, 110 8th Street, Troy, NY 12180, USA

Introduction: Hydrogen has attracted great attention as a source of secure, clean, sustainable energy and it is environmentally benign as it does not generate greenhouse gases [1]. Hydrogen is ubiquitous and it is often difficult to remove hydrogen from synthesis of nanomaterials. Therefore, studying interaction of hydrogen with metals and semiconductors is of immense interest owing to the development of efficient materials for the storage of hydrogen and gas-sensing devices. Ethanol has been suggested to be an efficient source of clean hydrogen after decomposition at high temperature or electrolysis at room temperature in the presence of metal and/or metal oxides. The intentional (or unintentional) doping of materials with hydrogen exhibits qualitatively different behavior depending on the host matrix [2]. Hydrogen can bind to the native defects and other impurities that are present in the host matrix and passivate their electrical activity. In contrast, bound hydrogen can also behave as a donor and increase the conductivity of the host matrix. The interaction of hydrogen with transparent conducting oxides has always been important to tailor their electrical and optical properties**.** High mobility hydrogen-doped In_2O_3 transparent conducting oxide has previously reported for use in high effficiency a-Si:H/c-Si hetero-junction solar cells. Although, in most of the semiconductors hydrogen counteracts the prevailing conductivity, the incorporation of hydrogen in oxides, such as In_2O_3 and ZnO, surprisingly results in donor activity (H+) and improves the electrical conductivity [3]. Hydrogen-doped indium oxide (IO) has been suggested as a better transparent conductor than the most commonly used tin doped IO. However, despite the importance and potential impact of IO on a large number of technological applications, there exists a lack of experimental studies that detail the microscopic behavior of such systems.

Experimental: In the present study the hydrogen-doped IO tubular nanostructures were synthesized by horizontal tube furnace maintained at a temperature of 1000°C, one atmosphere pressure and constant flow of argon carrier gas at the rate of 200 mL/min for 1 h. An alumina boat with a 1:1 mixture of IO and active carbon powder was placed at the center of the tube furnace while silicon substrates were placed downstream at a temperature of 960°C. A small reservoir (5-10 mL) of ethanol was placed in low temperature region (~65°C) in upstream direction during the growth. Ethanol acts as the source of hydrogen. The high diffusion coefficient of hydrogen results in the incorporation of hydrogen in IO nanostructures during the growth process. The samples were characterized by glancing angle X-ray diffraction (GAXRD) and high resolution transmission electron microscopy (HRTEM).

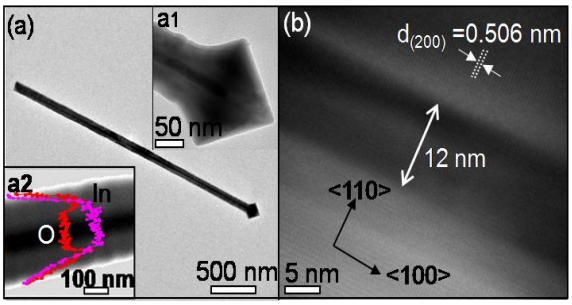

Results: Fig. 1(a) shows a TEM micrograph of a tubular IO nanostructure with a typical diameter of 95 nm and an octahedral tip with a radius of curvature as low as 5 nm at the end. The cavity and wall thickness of various IO tubular nanostructures vary from 10 nm to 60 nm and 35 nm to 100 nm, respectively. The HRTEM image of the tip region is shown as inset a1 of Fig. 1(a). The STEM-EDX measurement on IO tubular structure along its radial direction is shown in inset a2 of Fig. 1(a). The result confirms that the IO tubular nanostructures are filled with indium metal. Fig. 1(b) shows the lattice fringes of the two orthogonal planes of 0.506 nm and 0.71 nm, which correspond to (200) and (110) planes of IO shell, respectively. The HRTEM micrographs reveals that the tubular nanostructures grow along <100> direction. The hydrogen content in IO tubular nanostructures is measured at the FZD 5 MV Tandem accelerator by resonant nuclear reaction analysis $^{15}N(6.385\ MeV) + {}^{1}H \rightarrow {}^{12}C + {}^{4}He + \gamma$-rays (4.43 MeV). The hydrogen depth profile, shown in Fig. 2, is determined by gradually increasing the incident energy of ^{15}N ions and, thus, moving the resonance at 6.385 MeV ^{15}N ion energy progressively to greater depth.

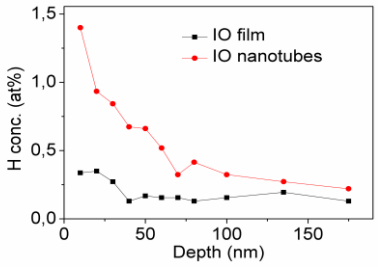

References: [1] Deluga G.A. et al. *Science* **303** (2004) 993. [2] de Walle C.G.V. and Neugebauer J. *Nature* **423** (2003) 626. [3] Koida T. et al. *Jpn. J. Appl. Phys*. **28** (2007) L685.

TEMPERATURE DEPENDENCE OF DAMAGE FORMATION IN Ag ION IRRAIDIATED 4H-SiC.
E. Wendler[1], Th. Bierschenk[1], W. Wesch[1], J.B. Malherbe[2] and E. Friedland[2], [1]Institut für Festkörperphysik, Friedrich-Schiller-Universität Jena, Max-Wien-Platz 1, 07743 Jena, Germany , [2]Department of Physics, University of Pretoria, Pretoria 0002, Republic of South Africa

Introduction: Modern high-temperature nuclear reactors are based on coated fuel particles. One coating component is SiC which acts as a main diffusion barrier for energetic fission products like e.g. iodine and silver (for details see e.g. [1]). In the present paper damage production in SiC is studied applying 360 keV Ag ions at various temperatures. The ion fluence was varied over a wide range allowing a careful analysis of the defect formation with special emphasis on very low fluences and the shape of the defect profiles.

Experimental: In this study <0001> oriented 4H-SiC samples were implanted with 360 keV Ag ions at a temperature of T_I = 15, 295, 375, 475, 625 or 875 K. Depending on the temperature, the ion fluence N_I varied between 1×10^{11} and 2×10^{16} cm^{-2}. Rutherford backscattering spectrometry in channelling mode was applied to measure the damage concentration after implantation, using 1.4 MeV He ions and a backscattering angle of 170°. The computer code DICADA [2] was applied to calculate the defect profiles from the Si part of the measured spectra. For comparison, the depth distribution of primary displacements and implanted ions were calculated with the computer code SRIM2008.04 [3].

Results: The results obtained for the various temperatures can be divided into two groups [4]: (i) For irradiation temperatures between 15 and 475 K amorphisation of the implanted layers is reached. The depth of maximum damage is constant, independent of the ion fluence applied, and agrees reasonably with the theoretical predictions of SRIM. (ii) For irradiations performed at 625 and 875 K no amorphisation is found for ion fluences as high as 2×10^{16} cm^{-2} and the depth of maximum damage coincides with the depth of maximum ion concentration.

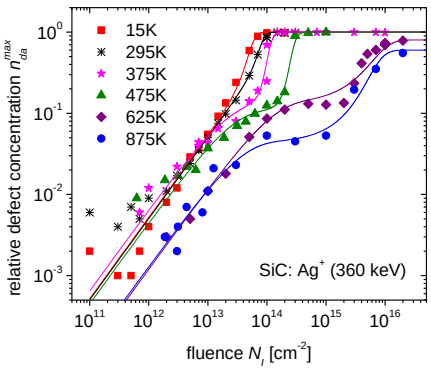

Fig. 1: Defect concentration in the maximum of the measured distribution, n_{da}^{max}, versus the ion fluence N_I for 360 keV Ag ion implantation in SiC at various temperatures. The lines are calculated with a defect-interaction and amorphisation model (for details see [4,5]).

A summary of the results is given in Fig. 1 which plots the defect concentration in the maximum of the measured distribution, n_{da}^{max}, as a function of the ion fluence for all implantation temperatures applied. The curves are fitted to the experimental data using a defect-interaction and amorphisation model which comprises the generation, recombination and stimulated growth of defects [4,5]).

Discussion: A significant change of the mechanisms of damage formation in 360 keV Ag implanted SiC occurs between 475 and 625 K. This range of temperatures coincides with that of annealing stages which may be attributed to the mobility of vacancies [4]. These mobile defects can promote the defect recombination within the collision cascades of individual ions, thus reducing the amount of damage remaining after implantation. At irradiation temperatures up to 475 K an almost equal over-all cross section of defect formation is obtained from the data at very low ion fluences for all temperatures in that range. This cross section involves the formation of point defects and amorphous clusters within a single ion impact. With rising temperature the transition to amorphisation shifts to higher ion fluences (see Fig. 1). This can be explained by a decrease of the relative amount of amorphous clusters within single ion impacts in crystalline SiC and by a reduced growth of already existing amorphous clusters [4]. Contrary, at temperatures of 625 and 875 K only point defects are produced. With rising ion fluence the balance between formation and recobination of point defects causes a plateau of the defect concentration over a wide range of fluences. A second step of damage formation is related to the increasing concentration of implanted ions in the implanted layer. A complicated defect structure, consisting of clusters of point defects and extended defects - most probably dislocations, starts to grow, which is supported by the mobility of intrinsic defects.

References: [1] Friedland E., Malherbe J.B., van der Berg N.G., Hlatshwayo T., Botha A.J., Wendler E., Wesch W. *J. of Nucl. Mater.* **389** (2009) 326. [2] Gärtner K. *Nucl. Instr. and Solids B* **227** (2005) 522. [3] Ziegler J.F., Biersack J.P., Littmark U. *The Stopping and Ranges of Ions in Solids, Pergamon, New York*, 2003; www.srim.org. [4] Wendler E., Bierschenk Th., Wesch W., Friedland E., Malherbe J.B. *Nucl. Instr. and Methods B*, in press. [5] Wendler E. *Nucl. Instr. and Methods B* **267** (2009) 2680.

CHARGE EXCHANGE RATES OF MeV-CARBON IONS IN ULTRATHIN CARBON FOILS.
R. Wiemann[1], M. Kosmata[1], M. Vieluf[1], D. Hanf[1], V.Kh. Liechtenstein[2], R. Grötzschel[1], W. Möller[1], [1]Institute of Ion Beam Physics and Materials Research, Forschungszentrum Dresden-Rossendorf, P.O. Box 510119, 01314 Dresden, Germany, [2]Russian Research Centre, "Kurchatov Institute, Kurchatov Sq., Moscow 123182, Russia

In recent years the Ion Beam Analytical (IBA) methods Rutherford Backscattering Spectrometry (RBS) and Elastic Recoil Detection (ERD) were further developed at FZD to achieve a depth resolution in the sub-nanometre range near the surface. There are several challenges to perform these high depth resolution methods.

To achieve that high depth resolution magnetic spectrometers are used, which disperse the momentum but also ion charges so that only one charge state is measured. Therefore, the charge state distribution of ions leaving the sample has to be known in order to quantify the measured data. Another problem is that the stopping power values, which are used to determine the depth of the scattering event, depend on the charge state of the ion.

For RBS and ERD with typical analysing depths up to several 100 nm the charge state distribution reaches equilibrium and an average is used for calculations [1]. However, typical analyzing depths in high-depth-resolution (HR-) RBS and ERD do not exceed 20 nm. Previous experiments using high-energy neon ions (44 MeV) traversing carbon foils of thicknesses between 20 and 250 nm [2] and our own *ab-initio* calculations suggest that these path lengths are so short that the non-equilibrium charge state distribution could have an influence on the depth scale determination.

For analysing the charge state distribution and the charge exchange processes, new set-up at FZD, the "banana" has been built. This set-up is similar to those described in [2,3].

In this work, we show this set-up and our results of charge exchange rates for carbon ions with an energy of several MeV in ultrathin carbon foils. These ions were guided through two foils to induce charge exchange and measured by an electrostatic analyzer. The thicknesses of the diamond like carbon foils are 2 µg/cm² for the first "stripper" foil and 0.5, 0.7 and 0.9 µg/cm² for the second "target" foil [4]. Due to the high content of sp^3-bonds these foils have a high stability. Hence, no disturbing grid support was needed to mount the foils over 100 µm holes. The first foil was used as an additional stripper to produce a full charge state distribution. This is necessary because the 5 MV-Tandem accelerator, equipped with a gas stripper, can only provide low charge states. Additionally, there is a potential difference between the two foils of 30 kV to separate charge states by energy steps of 30 keV. Next, the ions traverse the second foil and for every initial charge state we obtain a new charge state distribution. Last but not least, the ions were separated in an electrostatic analyser according to their charge states and their energies. Thus, the measured energy distribution corresponds to the initial charge state distribution before the second foil, and for each energy interval the measured charge state distribution corresponds to the final distribution.

Our results, illustrated in Fig. 1 show that the charge state equilibrium for 6 MeV carbon ions is already reached for the used foil thicknesses. However, it is not yet possible to produce thinner foils nor can higher energies be used with the existing set-up due to limitations of the electrostatic analyser. More detailed calculations show that the equilibrium is nearly reached after only 1 nm (see Fig. 1). So, the influence of non-equilibrium processes on the stopping power used in HR-IBA is insignificant after 1 nm. This makes it possible to use standard (equilibrium) stopping powers with only minimal errors.

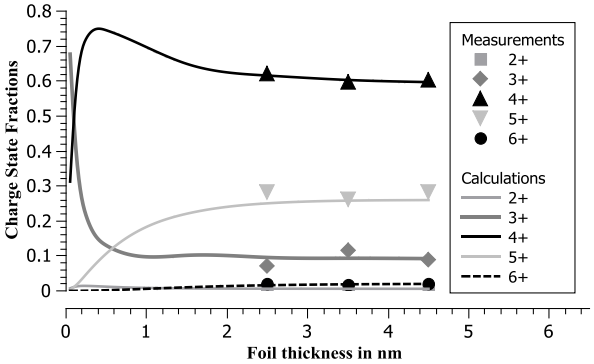

Fig. 1: Calculated evolution of the charge state fractions for incoming 6 MeV C^{3+} ions from the measured data under the assumption that only single charge exchanges took place.

References: [1] Ziegler J.F. *NIMB* 1027, 219-220 (2004) 1027. [2] Blažević A. et al. *Phys. Rev. A* **61** (2000) 32901. [3] Jiang W. et al. *Phys. Rev. B* **59** (1999) 226-234. [4] Liechtenstein V. Kh. et al. *NIMA* 397 (1997) 140-145.

EFFECT OF TEMPERATURE ON THE RETENTION OF 2 keV Cs^+ IONS IN Si. C. Wilde, W. Möller and J. Neidhardt, Forschungszentrum Dresden-Rossendorf, Institute of Ion Beam Physics and Materials Research, D-01314 Dresden, Germany

Introduction: Cesium is a commonly used species for SIMS, because it provides a high negative secondary ion yield. For more quantitative modeling of the secondary ion yield during SIMS the precise knowledge of the amount of Cs retained in the near surface region is vital. Its equilibrium concentration can be theoretically described by the implantation process and the material removal by (self) sputtering. However, the experimentally determined concentrations of Cs ions retained in Si [1] are lower than that predicted by TRIDYN or by the model of *Schulz* and *Wittmaack* [2]. This indicates more complex interaction of chemical (compound formation) or physical nature (texture), which is not described by the given models. The chemical incorporation of residual gas is thought to be a possible reason (e. g. [3]). Therefore, an IBA set-up including RBS and ERD for simultaneous in-vacuo detection of Cs and O in Si was developed to analyze the incorporation of oxygen during Cs sputtering as a function of sample temperature in order to draw conclusion of their activation threshold.

Set-up: The main chamber at the end of the ion beam line includes a resistively heated sample holder in focus of a Cs surface ionization source (Peabody Scientific PS-133) and a mass spectrometer (Hiden Analytics EQP1000). Both are mounted under an angle of 45° to the analyzing ion beam. Two semiconductor detectors (Canberra PD 150-16-100-AB) for RBS and ERD are installed under 150° and 28° to the analyzing ion beam. A 12 µm aluminated Mylar foil in front of the ERD detector stops heavy ions and decreases the depth resolution of O in Si to 30 nm.

Experimental: Sputter experiments were performed with 2 keV Cs^+ at normal incidence, for Si (100) sample temperatures up to 700°C. The ion beam current density was approx. 250 nA/cm². Areal densities of Cs and O were determined by a 38 MeV $^{35}Cl^{8+}$ beam, whereas the analyzing ion fluence and instrumental parameters were calibrated via a vane wheel using a 100 nm HfO_2 on Si reference sample. Sputtering and measurements were executed alternatingly.

Results: Figure 1 shows the saturation of Cs in Si at room temperature. The temporal development is consistent with the model of implantation and self sputtering. Regardless the low partial pressure of oxygen, there is also a strong correlation between Cs and O indicating ion-induced incorporation pathways on top of the natural oxide on the untreated Si surface.

Figure 2 shows the steady state areal densities for Cs and O as a function of temperature. Two discrete steady state regimes for Cs are observed at high (> 500°C) and low (< 250°C) temperatures with a transition, where the steady state areal density decreases almost linearly by a factor of four. The O concentration behaves congruently, while the deviation at temperatures > 600°C might be attributed to thermal oxidation.

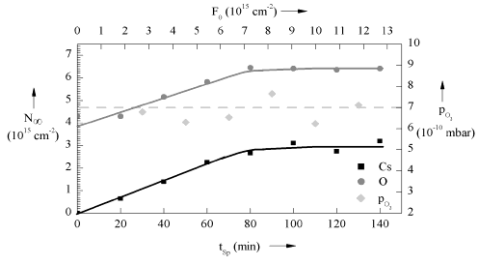

Fig. 1: Areal densities of Cs and O while sputtering with 2 keV Cs at normal incidence and room temperature.

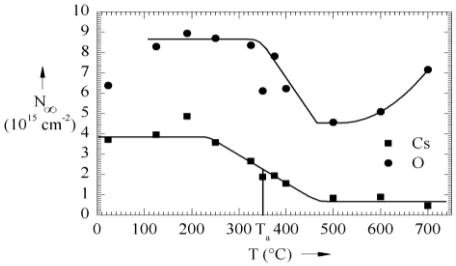

Fig. 2: Steady state surface concentrations of Cs and O for different temperatures for sputtering with 2 keV Cs at normal incidence.

Conclusion: Even though no significant influence on the physical conditions of the sputtering processes are expected within the temperature range, the Cs areal density shows two discrete regimes, which, interestingly, correlate closely to the amount of O incorporated from residual gas even at pressures below 10^{-7} mbar. The reported recrystallisation by rapid thermal annealing with an approx. 10% increase of sputter yield shown by *Anderson* [4] for Ar in Ge seems to be much too small to explain this strong decrease of steady state Cs concentration. Instead, overlying chemical processes are thought to play a major role, e. g. the Cs enhanced formation of mixed oxides (e. g. Cs_2O [5]) can impact sputtering yields and/or thermally desorb in the investigated temperature range under UHV conditions. Their precise nature remains unclear yet, but follow-up experiments at different O partial pressures might provide further insights.

References: [1] Gnaser H. *NIMB* **267** (2009) 2808. [2] Schulz F. and Wittmaack K. *Radiat. Eff.* **29** (1976) 31. [3] Berghmans B. and Vandervorst W. *J. Appl. Phys.* **106** (2009) 033509. [4] Anderson G. S. *J. Appl. Phys.* **38** (1967) 1607. [5] Michel E. G. et al. *Phys. Rev. B* **38** (1988) 13999.

SURFACE MODIFICATION OF KBr(001) WITH SLOW HIGHLY CHARGED IONS. R.A. Wilhelm, R. Heller, A.S. El-Said and S. Facsko, Forschungszentrum Dresden–Rossendorf, Institute of Ion Beam Physics and Materials Research, Bautzner Landstraße 400, 01328 Dresden, Germany, r.wilhelm@fzd.de

Highly Charged Ions (HCI) carry an enormous amount of potential energy (up to 100 keV for Xe^{50+}) which is defined as the sum of the binding energies of all missing electrons. This unique parameter offers new ways of surface modifications without a significant bulk damage.

During neutralization and de-excitation processes of the HCI the potential energy is released into electronic excitations within the solid (creation of electron hole pairs) [1]. These electron hole pairs get rapidly self-trapped due to strong electron-phonon coupling in the ionic lattice and decay into color centers (mainly H-, F- and F*-centers).

A H-center is an interstitial halide ion and a F-center is defined as an electron at an anion site. The diffusion of these color centers and their agglomeration at the surface may lead to desorption of neutralized K and Br atoms [2]. While the halide atom (Br) is weakly bound at the surface and thermally emitted, the recombination of the F-center with the surface is not sufficient enough to desorb the alkali atom (K) as long as the F-center remains in its ground state. However, F*-centers (2p-excited F-center) were found to have enough energy [3].

Desorption induced by electron transition (DIET) as described above is well known as a main process involved in sputtering from alkali halide surfaces by electrons (electron stimulated desorption - ESD) [4]. The DIET mechanism leads to the formation of pit-like structures due to electron bombardmet of alkali halide surfaces [5].

Similar pit-like structures can be observed after single HCI impacts due to the creation of a high local defect density in contrast to the cumulative formation of the pits during electron bombardment [6,7]. Fig. 1 shows pits on a KBr surface with a density which is in good agreement with the applied fluence.

In the case of surface modification due to HCI bombardment a certain threshold in the potential and kinetic energy was found to define a critical velocity-charge-state combination for pit-like structure creation on KBr as shown in Fig. 2.

This phenomena is known as kinetically assisted potential sputtering and was indentified by *Aumayr et al.* in 2001 (see [2]).

Recent results for KBr(001) surfaces irradiated with slow (< 300 eV/amu) highly charged (q > 20) Xe ions and analyzed with UHV contact-AFM will be presented.

The influence of kinetic and potential energy effects will be discussed.

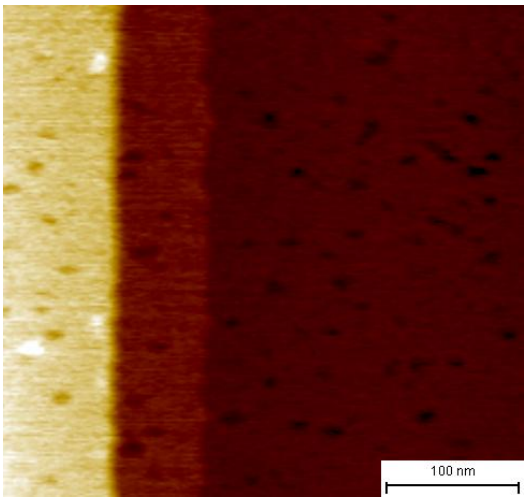

Fig. 1: Atomic Force Microscope (AFM) image of a KBr (001) surface irradiated with Xe^{25+} ions at a kinetic energy of 40 keV (287 eV/amu). Dark Spots indicate ion induced pit structures.

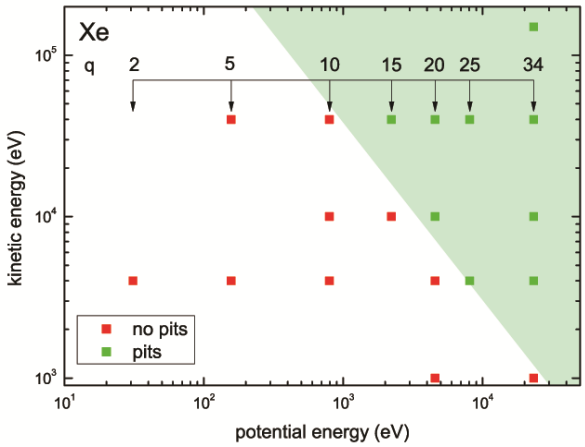

Fig. 2 Digram with velocity-charge-state combinations where pits were found (green) and no pits were found (red).

References: [1] Aumayr F. *IJMS* **192** (1999) 415-424. [2] Hayderer G. et al. *PRL* **86** (2001) 3530. [3] Puchin V. et al. *Phys. Rev. B* **46** (1994) 11364. [4] Ageev V.N. *Prog. Surf. Sci.* **47** (1994) 55-204. [5] Such B. et al. *PRL* **85** (2000) 2621. [6] Krog F. et al. *NIM B* **226** (2004) 601-608. [7] Heller R. et al. *PRL* **101** (2008) 096102.

IONS AND X-RAYS: UNIQUE PARTNERS FOR ACCURATE STOPPING POWER DETERMINATION OF ^{15}N IONS IN Si FOR HYDROGEN DEPTH PROFILING. M. Zier[1], U. Reinholz[2], H. Riesemeier[2], M. Radtke[2], F. Munnik[2], [a]Forschungszentrum Dresden-Rossendorf (FZD), D-01314 Dresden, Germany
[b]BAM Federal Institute for Materials Research and Testing, D-12200 Berlin, Germany

Introduction: In many areas of material sciences hydrogen analysis is of particular importance. For example, hydrogen is most abundant as impurity in thin-film materials - depending on the deposition process - and has great influence on the chemical, physical and electrical properties of many materials. Therefore, it is necessary to monitor the H-concentration by depth profiling. Best-suited methods for depth-resolved hydrogen analysis are ion beam techniques such as elastic recoil detection (ERD) and nuclear reaction analysis (NRA). In principle, both methods can be performed as primary - reference material free - methods.

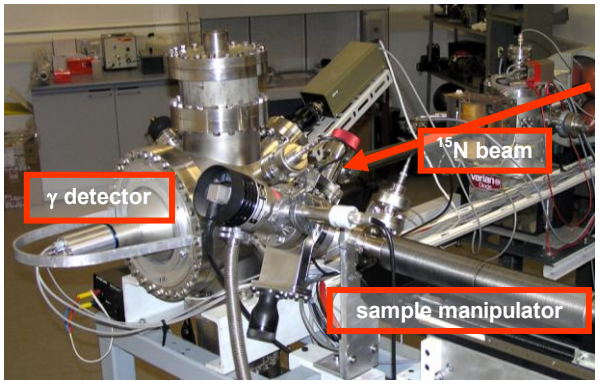

Fig. 1: NRA measurement chamber at FZD.

Experimental: The most common method, NRA, makes use of the 6.385 MeV resonance of the ^{1}H(^{15}N,αγ)^{12}C nuclear reaction [1]. The correct quantification of the depth scale in the measured hydrogen profiles essentially relies on accurate stopping power values, i.e. any imperfection in the stopping power values is influencing all H-values provided by NRA. For the determination of the accurate stopping power of ~6.4 MeV ^{15}N ions in hydrogen-containing amorphous Si-layers (a-Si:H), we have, therefore, combined NRA with X-ray reflectometry (XRR), also a primary method.

The samples are prepared by magnetron sputtering of a-Si in an Ar/H_2-atmosphere on a Cr-layer, which is needed as contrast material for XRR. The energy loss in the layers is measured by NRA at FZD (Fig. 1) [2]. The layer thickness, density and roughness are determined by XRR using synchrotron radiation. XRR measurements (Fig. 2) were performed at the electron storage ring BESSY at the hard X-ray beamline BAM*line* [3]. The beam was monochromatised to 10 keV using a Si [111]-double-crystal monochromator. The reflected photons of the θ-2θ-scans from the 6-circle goniometer are counted by a scintillation detector and a photodiode, respectively. Data analysis is performed by the IMD 4.1 software package [4].

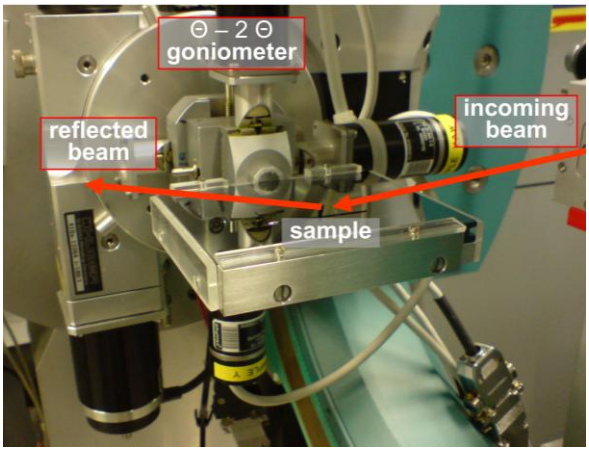

Fig. 2: 6-circle goniometer for XRR at BAM*line*.

The unique combination of results from NRA and XRR allows the accurate calculation of the mass stopping power independent of the density of the material.

Our results show a very good agreement with the commonly used stopping powers calculated by the well-accepted SRIM program (version 2006) [5], which indicates that this method is well-suited for re-evaluation of the stopping powers in other commonly used thin-film systems.

Acknowledgments: The help of D. Grambole and S. Merchel (FZD) is greatly appreciated.

References: [1] Lanford W.A. et al. *Appl. Phys. Lett.* **28** (1976) 566. [2] Wielunski L.S. et al. *Nucl. Instr. and Meth. B* **190** (2002) 693. [3] Görner W. et al. *Insight-Non-Destr. Test. Cond. Monit.* **48** (2006) 540. [4] Windt D.L. *Comp. in Physics* **12** (1998) 360. [5] Ziegler J.F. *Nucl. Instr. and Meth. B* **219-220** (2004) 1027. URL: http://www.SRIM.org.

ION BEAM CHARCTERISATION AND DEVELOPMENT AT DRESDEN EBIS/T. E. Ritter[1*], J. König[1], A. Thorn[1], G. Zschornack[1], U. Kentsch[2], V. Ovsyannikov[2], M. Schmidt[2], A. Schwan[2] and F. Ullmann[2], [1]Technical University of Dresden, Institute of Applied Physics, 01062 Dresden, Germany, [2]DREEBIT GmbH, Zur Wetterwarte 50, Haus 301, 01109 Dresden, Germany, * e.ritter@fzd.de

Measurements of the longitudinal and the transversal emittance of a Dresden EBIS-A are presented. Therefore a new retarding field analyzer and a pepper pot emittance meter were developed. With a root mean square emittance lower than 10 mm mrad and an energy spread of lower than 0.15 eV/u the excellent beam parameter are demonstrated. Furthermore, new developments in the area of ion source evolution are shown. A shorter extraction lens system in combination with a ExB-Filter (Wien-Filter) results in a very compact system producing a charge state separated beam of highly charged ions. Preliminary results from the new EBIS-SC are figured out as well.